



**HAL**  
open science

## Acoustic Properties of Aerogels: Current Status and Prospects

Tatiana Budtova, Tapio Lokki, Sadeq Malakooti, Ameya Rege, Hongbing Lu, Barbara Milow, Jaana Vapaavuori, Stephanie L Vivod

► **To cite this version:**

Tatiana Budtova, Tapio Lokki, Sadeq Malakooti, Ameya Rege, Hongbing Lu, et al.. Acoustic Properties of Aerogels: Current Status and Prospects. *Advanced Engineering Materials*, 2022, pp.2201137. 10.1002/adem.202201137 . hal-03903918

**HAL Id: hal-03903918**

**<https://hal.science/hal-03903918v1>**

Submitted on 16 Dec 2022

**HAL** is a multi-disciplinary open access archive for the deposit and dissemination of scientific research documents, whether they are published or not. The documents may come from teaching and research institutions in France or abroad, or from public or private research centers.

L'archive ouverte pluridisciplinaire **HAL**, est destinée au dépôt et à la diffusion de documents scientifiques de niveau recherche, publiés ou non, émanant des établissements d'enseignement et de recherche français ou étrangers, des laboratoires publics ou privés.

# Acoustic Properties of Aerogels: Current Status and Prospects

Tatiana Budtova,\* Tapio Lokki, Sadeq Malakooti, Ameya Rege, Hongbing Lu, Barbara Milow, Jaana Vapaavuori, and Stephanie L. Vivod

Noise reduction remains an important priority in the modern society, in particular, for urban areas and highly populated cities. Insulation of buildings and transport systems such as cars, trains, and airplanes has accelerated the need to develop advanced materials. Various porous materials, such as commercially available foams and granular and fibrous materials, are commonly used for sound mitigating applications. In this review, a special class of advanced porous materials, aerogels, is examined, and an overview of the current experimental and theoretical status of their acoustic properties is provided. Aerogels can be composed of inorganic matter, synthetic or natural polymers, as well as organic/inorganic composites and hybrids. Aerogels are highly porous nanostructured materials with a large number of meso- and small macropores; the mechanisms of sound absorption partly differ from those of traditional porous absorbers possessing large macropores. The understanding of the acoustic properties of aerogels is far from being complete, and experimental results remain scattered. It is demonstrated that the structure of the aerogel provides a complex three-dimensional architecture ideally suited for promising high-performance materials for acoustic mitigation systems. This is in addition to the numerous other desirable properties that include low density, low thermal conductivity, and low refractive index.


## 1. Introduction

Noise pollution has been aptly described as one of the modern plagues.<sup>[1]</sup> Due to many adverse health effects of loud environments, ranging from sleep disturbances to cardiovascular diseases, reducing the exposure of humans to excess noise is essential to the public health of large populations living in the cities. Regarding sound absorption materials, the optimal choice depends on the intended sound frequency range; solutions of damping high-frequency sound waves rely on totally different absorption mechanism than the solutions for very low-frequency noise. Indoors, the most commonly used sound absorption materials are porous by nature due to their ability to efficiently absorb sound at mid to high frequencies with relatively thin layers. Common porous absorption materials in the market, targeting to over 90% absorption above 350 Hz, are glass and mineral wools and acoustic foams made, e.g., from melamine or polyurethane. Here, we review the acoustic

properties of aerogels and demonstrate their high potential to challenge and exceed the absorption properties of the current market standards, whether we talk about the performance in

T. Budtova  
MINES Paris  
PSL University  
Center for Materials Forming (CEMEF)  
UMR CNRS 7635  
CS 10207, 06904 Sophia Antipolis, France  
E-mail: tatiana.budtova@minesparis.psl.eu

T. Lokki  
Department of Signal Processing and Acoustics  
Aalto University  
02150 Espoo, Finland

 The ORCID identification number(s) for the author(s) of this article can be found under <https://doi.org/10.1002/adem.202201137>.

© 2022 The Authors. Advanced Engineering Materials published by Wiley-VCH GmbH. This is an open access article under the terms of the Creative Commons Attribution-NonCommercial License, which permits use, distribution and reproduction in any medium, provided the original work is properly cited and is not used for commercial purposes.

DOI: 10.1002/adem.202201137

S. Malakooti, S. L. Vivod  
NASA Glenn Research Center  
Materials and Structures Division  
21000 Brookpark Rd, Cleveland, OH 44135, USA

A. Rege, B. Milow  
Department of Aerogels and Aerogel Composites  
Institute of Materials Research  
German Aerospace Center (DLR)  
Linder Höhe, 51147 Cologne, Germany

H. Lu  
Department of Mechanical Engineering  
The University of Texas at Dallas  
Richardson, TX 75080, USA

J. Vapaavuori  
Department of Chemistry and Material Science  
Aalto University  
02150 Espoo, Finland

acoustic absorption or aspects related to their processability or sustainability.

The term “aerogel” should first be defined as literature often provides different approaches. According to IUPAC Gold Book, aerogel is a “Gel comprised of a microporous solid in which the dispersed phase is a gas” with “microporous silica, microporous glass and zeolites” given as examples.<sup>[2]</sup> This definition is very restrictive as it includes only microporous materials, i.e., with pore sizes below 2 nm, and thus excludes, for example, classical silica aerogels that have pores from a few to a few dozens of nanometers. It is now commonly agreed that aerogels are open cell porous networks with high porosity (at least 90%), high specific surface area (approximately, higher than  $100\text{ m}^2\text{ g}^{-1}$ ), and are nanostructured (mainly mesoporous with small macropores).

The classical way of making aerogels is extraction of the fluid from the pores of a gel via drying with supercritical  $\text{CO}_2$ . In some cases, freeze-drying may also result in lightweight high specific surface area materials. However, in the majority of cases, freeze-drying is performed by sublimation of ice formed in the pores of a gel; such procedure usually results in very large macropores that are replicas of ice crystals. In this context, freeze-dried materials will be called “cryogels” for simplicity. If the fluid in the pores of gels is extracted at ambient pressure or under low vacuum evaporative drying, high capillary pressure, which develops during drying, usually results in the collapse of the pores. These materials will be called “xerogels”; they are usually with rather high density and low specific surface area. An exceptional case is ambient-pressure dried silica gels: silylation of silica helps the preservation of gel morphology after ambient pressure drying, resulting in aerogel-like materials.<sup>[1]</sup> In this review, we will focus on “aerogels” within the definition given above and based on all types of matter. The examples of acoustic properties of cryogels and xerogels, as well as of other porous materials, will also be given for comparison.

In addition to common fibrous sound absorption materials, nanofibrous electrospun mats are considered to be promising for noise reduction.<sup>[2]</sup> Compared to felts based on micron-size fibers, nanofiber-based electrospun materials have better acoustic performance due to the increased internal surface area and friction and vibration of nanofibers.<sup>[3]</sup> The majority of electrospun materials are based on polyvinylidene fluoride due to its piezoelectric properties and ability to convert acoustic energy into electric potential.<sup>[4]</sup> Other synthetic polymers (polyacrylonitrile, polyvinyl pyrrolidone, polyvinyl acetate, etc) and their composites with inorganic compounds have also been used for electrospinning.<sup>[5]</sup> In most cases sound is absorbed in low- and middle-frequency regions with sound absorption coefficient reaching 0.8–0.9 values at 600–1000 Hz.<sup>[6]</sup> Despite fibers’ diameter in sub-micron range and high porosity of electrospun mats (see, for example,<sup>[3,7]</sup>), their pore sizes are within large macropores range (unless a special treatment is used to make fibers themselves mesoporous or microporous), and specific surface area remains low as compared to aerogels: around few tens versus several hundreds of  $\text{m}^2\text{ g}^{-1}$ , respectively. Because electrospun mats are, by far, macroporous, their acoustic properties can be predicted, to some extent, by theoretical sound absorption models. As it will be shown in this review, this is not the case for aerogels possessing mesoporous (and small macropores) morphology which makes them a special class of materials.

As a consequence, the acoustic properties of electrospun mats as well as other highly macroporous materials will not be discussed in this review.

Absorption of sound energy by porous materials occurs through the interconnected pores due to viscous, thermal, and inertial effects caused by the interaction of air molecules at the interfaces of the gas and the solid phases. For efficient sound energy dissipation in a porous material, geometry of a solid frame should be designed in such a way that the interactions of air molecules with the frame are maximized. In other words, the size of the pores should be large enough that the sound waves penetrate deeply into the material, but small enough to maximize the number of encounters of the gas with the boundaries. In dry air (0% humidity) at normal atmospheric pressure, the mean free path of an air molecule before colliding with another one is 66 nm.<sup>[8]</sup> This means that the likelihood of an air molecule to enter pores smaller than this value is reduced, and they can interact only with the surface of the frame. In other words, the nano-scale porous structures would appear as “homogeneous” to air molecules. Therefore, in general, the size of the pores is supposed to be above few hundreds of nanometers to let the air molecules penetrate deeply into the material for maximizing the interactions with pore walls, i.e., transforming the sound energy into heat. A more detailed description of sound absorption mechanisms in materials having structural characteristics dimensions below  $1\text{ }\mu\text{m}$  is presented in the next section. It is important to emphasize that the understanding of these mechanisms is still at its infancy.

Consequently, fabricating materials with optimized combination of density and pore sizes should lead into exceeding the sound absorption properties of conventional absorbents. Aerogels, as materials exhibiting very high specific surface area, can, potentially, increase all three sound attenuation mechanisms, namely inertial, viscous, and thermal effects. The increase in the specific surface area and tortuosity hamper most effectively the movement of air, i.e.,  $\text{O}_2$  and  $\text{N}_2$  molecules. We assume that the absorption mechanisms in aerogels differ significantly from the traditional porous acoustic materials, as usually the focus has been on the bulk effects that are caused by macroscopic structures. For example, high surface area materials, e.g., activated carbon, have been shown to have peculiar sound absorption properties especially at the low frequencies.<sup>[9]</sup> Generally, as discussed in this review, the establishment of the understanding of the relationship between the morphology of a highly porous nanostructured material with high specific surface area and their sound absorption properties will require more theoretical, computational, and experimental contributions.

Another important aspect, when aiming for resource-wise societies, is the sustainable production of high-performance sound absorption materials. The field of bio-based and sustainable sound absorbing materials has gained interest in the recent years,<sup>[2,10]</sup> but there is no large-scale production of acoustic materials made out of natural polymers. In fact, taken into account the estimated value of the acoustic insulator market size based on conventional materials, 15 billion USD by 2022,<sup>[11]</sup> there is a huge demand for novel materials that are environmental-friendly, nonhazardous, resistant to hostile environments (high temperatures or hits, among others), economical, esthetic, and of reduced thickness. We believe that a thorough life-cycle

assessment of proof-of-a-concept sound absorbents is required to identify how their sustainability can be increased. In any event, the development of novel materials and implementation of circular economy approaches should allow overcoming the sustainability problems of current market standards, glass and mineral wool, as well as polyurethane foams.

The goal of this review article is to summarize what is known about the acoustic properties of various aerogels: silica, synthetic polymer, organic/inorganic composites, and bio-based. First, we set the general background of the acoustic properties of porous materials. Then we introduce different types of aerogels, their synthesis, morphology, and main properties. Afterward, we analyze the results known in literature on each type of aerogels mentioned above. Finally, we summarize the potential of using aerogels for acoustic insulation.

## 2. Background on Acoustic Properties of Porous Materials

The attenuation of sound in porous materials is mainly based on viscous, thermal, and inertial effects, which results in the transfer of the acoustic energy into heat. In addition, structural damping could increase the attenuation at some frequency range, and such needs have intensified the design of sound absorbers with a specific resonating structure(s), e.g., periodic slits or holes, see, for example, Zangeneh-Nejad and Fleury.<sup>[12]</sup> Sound waves penetrating the porous medium set air molecules, mainly O<sub>2</sub> and N<sub>2</sub>, within the pores into oscillation. The interaction between the gas and the solid frame causes sound energy losses by three different main mechanisms: 1) viscous losses are caused by the generation of shear forces, also known as viscous stresses, that aim to equate the velocity of the two media by transferring some of the gas' kinetic energy into heat. Viscous forces have the effect of increasing the effective density of the gas traveling through the pores. In porous materials, viscous forces depend on the geometry of the pores, dynamic viscosity of the gas, and the contact surface available for the gas to interact with pore walls. The viscous boundary layer is the area in which viscous forces efficiently attenuate sound energy. The sound velocity within the viscous boundary layer is minimum at the surface of the rigid frame, where the effect of viscous forces is maximum. The speed of the gas increases with distance from the surface and reaches its maximum outside the boundary layer. The dimensions of the viscous boundary are greater at lower frequencies than at higher frequencies, from about 350 to 10 μm in the audible frequency range. Consequently, sound energy attenuation due to viscous stresses is more significant at lower frequencies.<sup>[13]</sup> 2) molecules from the gas are hitting the pore walls when entering a porous material. During this short time, there is an energy exchange that aims at thermal equilibrium between the gas and the solid frame.<sup>[13]</sup> After the exchange of energy, molecules are released with a modification in the magnitude of their velocity, thus reducing the sound energy. Analogously to the viscous boundary layer, the area where the molecules of the gas and the solid exchange thermal energy is known as thermal boundary layer. The thickness of the thermal boundary layer is of the same range as the viscous boundary layer, although it depends on the thermal properties of

the gas and the material of pore walls, and on the sound frequency. Even though at high frequencies the boundary layer is very small, in high specific surface area structures, thermal boundary layer might still be significant; and 3) the third main mechanism for energy losses can be explained by the inertial effects or exchange of momentum between the molecules of the gas.<sup>[13]</sup> A process of energy exchange is initiated when gas molecules impact the pore walls.

Summarizing the existing literature on acoustic absorption, where the concept of a "porous material" refers to materials with pore sizes of several orders of magnitude larger than those in the aerogels, viscous, and thermal losses dominate at low frequencies. At high frequencies, the inertial effects dominate as the viscous and thermal boundary layers are so thin that their effect on sound absorption is negligible. Viscous and inertial losses result in an increase in the effective density of the gas within the porous materials. Furthermore, thermal losses are substantial at low frequencies, where sound propagation is considered as an isothermal process, which involves thermal exchange between the gas and the pore walls. At high frequencies, sound absorption is considered as an adiabatic process, as compressions and rarefactions happen so fast that there is no time for the heat transfer.

Modeling the sound absorption in the materials such as aerogels is extremely challenging as the existing theories are adapted to materials with much larger pores. Moreover, the direct generalization related to the dominance of different absorption mechanisms in aerogels cannot be made, for the same exact reason. It might even be possible to design an aerogel with such lightweight pore walls that they could vibrate, adding one more sound absorption mechanism.

When characterizing the sound absorption properties of a material, the key value is sound absorption coefficient. The most common way of measuring this on a benchtop scale is to use an acoustic impedance tube. The sample sizes vary from a dozen millimeters to 100 mm and with the measurement method defined in the ISO 10534-2 standard the incoming and outgoing sound waves can be separated allowing the analysis of energy fraction absorbed by the material. The drawback of this method is that only the perpendicular wave direction can be studied. For the diffuse field sound absorption measurement, defined in the ISO 354 standard, the requirement for a sample size is 10 m<sup>2</sup> and a special purpose reverberation room. Therefore, measurement of the absorption coefficient in the diffuse sound field is out of the reach for aerogel samples. Unfortunately, current literature often does not use standards for sound absorption characterization making the comparison of different materials produced at different locations quite difficult.

## 3. Background on Aerogels: Inorganic, Synthetic Polymer, Bio-Aerogels—Main Principles of Synthesis and Overview of Their Structure and Properties

Aerogels are materials with very low density (below 0.2 g cm<sup>-3</sup>, usually around 0.01–0.1 g cm<sup>-3</sup>), nano-scale pore sizes, and with high porosity (>90%). What makes aerogels different from other

porous materials such as foams and sponges is their very high specific surface area, at least above  $100 \text{ m}^2 \text{ g}^{-1}$ , and even up to several thousand  $\text{m}^2 \text{ g}^{-1}$ .<sup>[14]</sup>

The first aerogels were synthesized by Kistler in 1931 who removed the liquid from a gel (inorganic oxides and some bio-based matter) via drying in supercritical  $\text{CO}_2$ ; as a result, a solid, open-pores network that maintained the 3D structure of the gel was obtained.<sup>[15,16]</sup> In the following decades, the research on aerogels was minimal until the 1970s when S. Teichner suggested a new preparation route for silica aerogels, from tetraethyl orthosilicate (TEOS) sol in ethanol.<sup>[17]</sup> This significantly reduced the time of aerogels' synthesis and improved their properties. Next, aerogels based on metal oxides were synthesized.<sup>[18]</sup> A significant step forward in the development of silica aerogels was done when functionalization (silylation) of the gel network allowed the preservation of gel morphology after ambient pressure drying: aerogel-like materials with low density and very high specific surface area were obtained.<sup>[1]</sup> However, monolithic gels break under such drying into subcentimeter particles due to the so-called "spring-back effect," i.e., contraction and subsequent re-opening of the pores at the final stage of drying due to the repulsion of the grafted groups.<sup>[1]</sup> The last decade of the 20th century was marked by the development of aerogels based on synthetic polymers: first resorcinol-formaldehyde<sup>[19]</sup> and later polyamide,<sup>[20]</sup> polyimide,<sup>[21]</sup> and polyurethane.<sup>[22]</sup> Finally, aerogels based on polysaccharides and proteins, so-called bio-aerogels, started to be investigated from the beginning of the 21st century.<sup>[23,24]</sup> The preparation, structure, properties, and applications of various aerogels are summarized in Aerogels Handbook.<sup>[14]</sup>

The main principles of the preparation of aerogels are shown in **Figure 1**. Two main options should be considered: the starting matter is 1) a solution of monomers (case of synthetic polymer aerogels) or a sol of inorganic precursors (case of inorganic

aerogels), Figure 1a and 2) solution or suspension of a natural polymer (polysaccharide, protein), Figure 1b,c, respectively. The fundamental difference between the two options is that in the case of synthetic polymer or inorganic aerogels the process starts with polymerization while in the case of biopolymers no polymerization, and often even no gelation or cross-linking, is needed. The common point for all aerogels is that in the majority of cases, drying with supercritical  $\text{CO}_2$  is necessary to avoid pore collapse arising from capillary stresses. Ambient pressure drying, resulting in aerogel-like material with high specific surface area and porosity, has been developed, till now, for silica aerogels, and, very recently, for cellulose and some synthetic polymer aerogels.<sup>[25–27]</sup>

The first silica aerogels were made from aqueous sodium silicate ( $\text{Na}_2\text{SiO}_3$ ), also called "water glass," which is gelling in the presence of an acid, usually  $\text{HCl}$ .<sup>[16]</sup> As a salt (here,  $\text{NaCl}$ ) is formed during this reaction, it must be eliminated by a dialysis or using ion exchanges. Nowadays, alkoxides ( $\text{SiOR}_4$ ), which are soluble in ethanol, are used to make silica-based aerogels. R is often either a methyl group ( $\text{CH}_3$ ) with the precursor tetramethoxysilane (or TMOS) or ethyl group ( $\text{C}_2\text{H}_5$ ) with the precursor tetraethoxysilane (or TEOS) or other silica derivatives such as methyltrimethoxysilane (MTMS), dimethyldiethoxysilane, etc. In all these cases, "polymerization" occurs via hydrolysis and polycondensation, with gelation often speeded up by the addition of a catalyst, either a basis (often  $\text{NH}_3$ ) or an acid (often  $\text{H}_2\text{SO}_4$ ). The advantage of using alkoxides is that no solvent exchange is needed for drying with supercritical  $\text{CO}_2$ . Before drying, often aging and/or cross-linking is performed to improve the mechanical properties of the gel and of the subsequent aerogel (Figure 1a). Hydrophobization or other types of silica functionalization can also be made before drying.

A similar sol-gel approach is applied for the synthesis of other inorganic aerogels, e.g., based on zirconium, titania, and

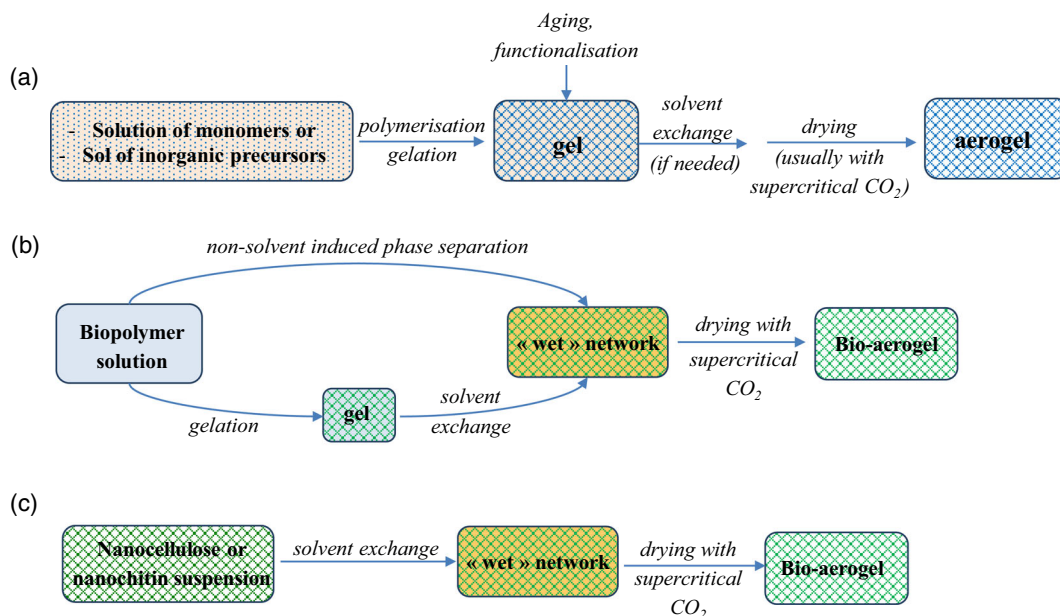


**Figure 1.** Main approaches of the preparation of aerogels: a) case of synthetic polymer and inorganic precursors, b) case of solutions of natural polymers,<sup>[23]</sup> and c) case of suspensions of natural nanoparticles.

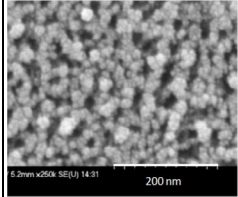
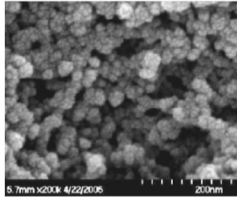
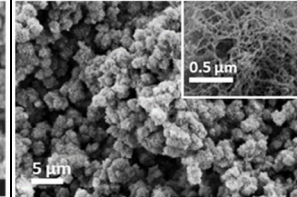
transition metal alkoxides (Figure 1a). Templating with surfactants or polymers followed by posttreatment (annealing) is sometimes performed to diversify aerogel morphology. Drying can be performed either under classical low-temperature or high-temperature supercritical conditions resulting in aerogels with different crystallinity. Aerogels can be doped by metals (platinum, iron, and copper) or by ions (sulfate, phosphate, and tungstate anions) for making materials with catalytic properties. Simple inorganic metal salts (metal nitrates or halides) can also be used for synthesizing inorganic aerogels applying epoxide-initiated gelation with organic epoxides as initiators. This approach allows synthesizing interpenetrated networks of the two metal oxides.

The first organic aerogels were synthesized from resorcinol-formaldehyde,<sup>[19]</sup> utilizing the same route as silica gels, whereby the reaction occurs via base-catalyzed or acid-catalyzed polycondensation, here, of resorcinol with formaldehyde in an aqueous medium. This approach was then extended to other formaldehyde-based networks such as phenol-formaldehyde or melamine-formaldehyde. Nowadays, numerous synthetic polymer aerogels based on polyimides, polyacrylamides, polyacrylonitriles, polyacrylates, polystyrenes, and polyurethanes have been synthesized. For example, polyurethane gels were synthesized by polycondensation in organic solvents<sup>[28]</sup>; standard catalysts employed for the synthesis of polyurethanes, i.e., metal salts or tertiary amines, can be used. Polymer-inorganic composite aerogels were also developed: they are based either on the “independent” interpenetrated networks or when organic and inorganic parts are linked by various types of bonds. For example, amine-functionalized silica was cross-linked with polyfunctional isocyanates or epoxides or polystyrene.<sup>[29]</sup>

Bio-aerogels can be made either from a polymer solution (Figure 1b) or, in the case of nanocellulose and nanochitin, from a suspension of “nanoparticles” (nanofibers or nanocrystals) (Figure 1c). If the starting matter is biopolymer solution (polysaccharide, protein), it can be gelled or not; in the latter case the morphology and macroscopic shape of the future aerogel is fixed via nonsolvent induced phase separation (or immersion

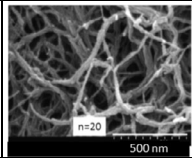
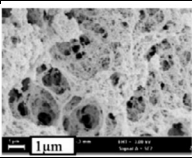
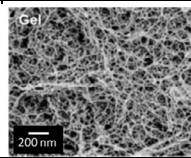
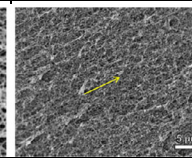
precipitation). Gelation can occur either via chemical cross-linking or physical reversible bonds. Depending on the external conditions, the same polymer can form different types of networks: for example, at low pH pectin solutions are gelling via hydrogen bonds between protonated carboxyl groups and/or via hydrophobic interactions; at pH around and above, pKa pectin solutions can be cross-linked with calcium ions, and pectin solutions can also form a network of coagulated polymer upon the addition of a nonsolvent (ethanol or acetone).<sup>[30]</sup> Bio-aerogel structure and properties depend on the network formation pathway. Solvent to nonsolvent exchange is, in any case, needed, as in the majority of cases the solvent of a biopolymer (solution or gel) is not miscible with CO<sub>2</sub>. This also applies to the case of nanocellulose and nanochitin for which the dispersing medium is usually water. Here the morphology and shape can be stabilized by the addition of a nonsolvent without chemical cross-linking. Finally, in a few cases, a polysaccharide can be dissolved in a solvent miscible with CO<sub>2</sub>: for example, aerogels were synthesized from cellulose diacetate or cellulose acetate butyrate that were dissolved in acetone and cross-linked with isocyanates.<sup>[31]</sup> This synthesis pathway can be seen as being similar to that of (poly) urethane-based aerogels, but the starting matter is polymer versus monomer solution, respectively.

Two main types of morphologies can be detected on SEM images of aerogels: either bead-like (Figure 2) or net-like (Figure 3). Classical silica aerogels are known to form a hierarchical “pearl necklace” network made of nonporous primary particles of diameter below 1 nm interconnected to form porous secondary particles of diameter around 5–10 nm linked by thin “necks,” resulting in fragile mechanical properties (Figure 2a). Resorcinol-formaldehyde aerogels also possess a bead-like morphology (Figure 2b); on a larger scale, bead-like morphology was reported for aerogels made from cellulose dissolved in ionic liquids (Figure 2c). However, opposite to silica aerogels, the internal morphology of these “internal” cellulose beads is a network of fine fibers (see inset in Figure 2c). Despite visually similar morphology and bulk density (around 0.13–0.17 g cm<sup>-3</sup>), the specific surface area is very different (the highest for silica

	Silica aerogel	Resorcinol-formaldehyde aerogels	Cellulose aerogel from cellulose dissolved in 1-ethyl-3-methylimidazolium acetate/dimethyl sulfoxide (no gelation)
			
Density, g/cm <sup>3</sup>	0.17	0.175	0.13
Specific surface area, m <sup>2</sup> /g	997	440	282

**Figure 2.** Examples of aerogels with bead-like morphology: silica aerogel,<sup>[115]</sup> (Reprinted with permission.<sup>[115]</sup> Copyright 2007, American Chemical Society), resorcinol-formaldehyde aerogel<sup>[115]</sup> (Reprinted with permission.<sup>[115]</sup> Copyright 2007, American Chemical Society), and cellulose aerogel<sup>[116]</sup> (Reprinted by permission from Springer.<sup>[116]</sup> Copyright 2016).



	Cross-linked polyimide aerogel	Cellulose aerogel from cellulose dissolved in 8%NaOH-water and gelled	Pectin aerogel from pectin solution (at pH 3), cross-linked with calcium	Nanofibrillated cellulose aerogel
				
Density, g/cm <sup>3</sup>	0.1	0.117	0.09	0.01
Specific surface area, m <sup>2</sup> /g	240-260	220	500	550

**Figure 3.** Examples of aerogels with net-like morphology: cross-linked polyimide,<sup>[21]</sup> (Reprinted with permission.<sup>[21]</sup> Copyright 2011, American Chemical Society), cellulose aerogel,<sup>[117]</sup> (Reprinted by permission.<sup>[117]</sup> Copyright 2014, Springer), pectin aerogel<sup>[52]</sup> (Reprinted from,<sup>[52]</sup> Copyright 2018, with permission from Elsevier), and nanofibrillated cellulose aerogel<sup>[54]</sup> (Reprinted by permission.<sup>[54]</sup> Copyright 2014, Wiley-VCH).

aerogel and the lowest for cellulose aerogel, see Figure 2), and polymer-based aerogels are mechanically much stronger than the silica ones.

The examples of aerogels with net-like morphology are shown in Figure 3, all for aerogels based on polymers: polyimide, cellulose (dissolved in 8%NaOH-water and gelled), pectin (cross-linked with calcium), and nanofibrillated cellulose. Depending on the synthesis conditions, the fibrils in some synthetic polymer aerogels (polyimide, polyurea) may have a “caterpillar” morphology (not shown, see, for example,<sup>[32,33]</sup>).

The mechanical properties of aerogels strongly depend on the type of matter and network structure. Classical silica aerogels are known to be very brittle because of the weak links between the nanoparticles’ “necks” in the “pearl necklace” structure (see Figure 2). As measuring the mechanical properties of brittle materials is complicated, the majority of experiments are performed under the uniaxial compression. It should be noted that the mechanical response depends on the applied strain rate. At

low loading rate, the stress–strain dependence of silica aerogels under compression is similar to that of foams with elastic (usually very small), plastic, and densification regions, at high strain rates cracks develop and silica aerogels break. The compressive modulus of silica aerogels  $E$  is from few hundreds of kPa to few MPa at bulk density  $\rho_{\text{bulk}}$  around 0.1–0.2 g cm<sup>-3</sup> (see, for example,<sup>[34,35]</sup>). To improve their mechanical properties, in particular, toughness, crosslinking is applied. This may lead to one order of magnitude increase in the modulus (Figure 4).<sup>[34–36]</sup>

Synthetic polymer aerogels, for example, based on resorcinol-formaldehyde, are not brittle and follow foam-like stress–strain dependence (Figure 4b);<sup>[37]</sup> similar trends were reported for other polymer aerogels.<sup>[33,38,39]</sup> Compressive modulus of synthetic polymer aerogels can reach several tens of MPa at density around 0.1–0.2 g cm<sup>-3</sup>.

For classical open-cell foams, it was demonstrated that modulus scales with bulk density

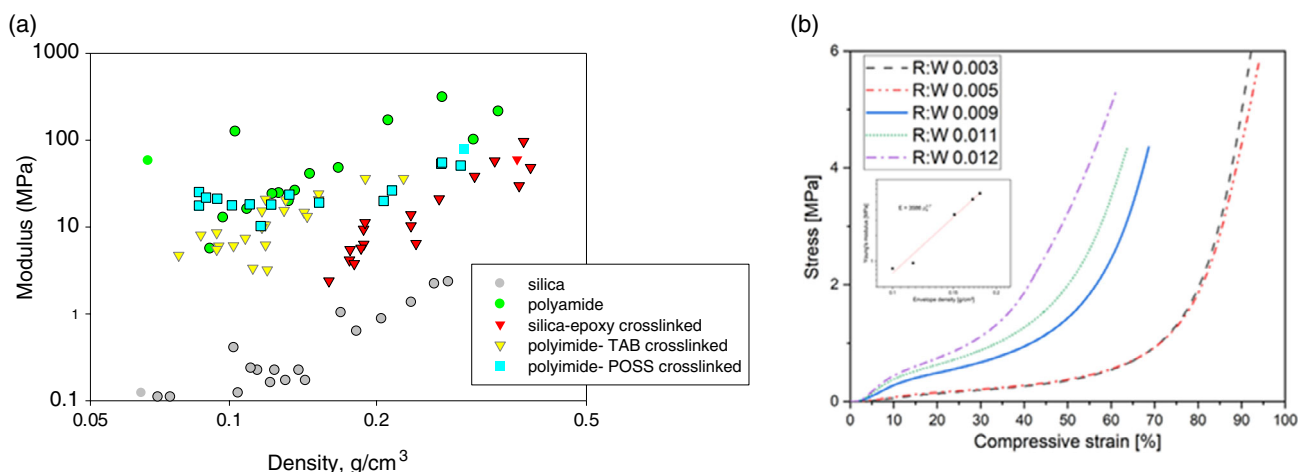


**Figure 4.** Illustration of the mechanical properties of aerogels: a) compressive modulus of various aerogels as a function of density (TAB is 1,3,5-benzenetricarbonyl trichloride, POSS is polyhedral oligomeric silsesquioxane), data taken from;<sup>[20,35,97,118]</sup> b) stress–strain curves stress–strain for resorcinol–formaldehyde aerogels under compression displaying the dependence on the resorcinol (R):water (W) ratio. Reproduced with permission.<sup>[37]</sup> Copyright 2021, The Authors, published by Wiley-VCH.

$$E \propto \rho_{\text{bulk}}^m \quad (1)$$

with  $m = 2$  for open-cell foams<sup>[40]</sup> and  $m = 3 - 4$  for silica and synthetic polymer aerogels<sup>[41–43]</sup>. Data for polysaccharide-based aerogels scatter a lot. Stress–strain dependences are “foam-like” as for aerogels based on synthetic polymers;<sup>[44]</sup> however, the scaling exponent varies significantly depending on the polysaccharide and on network morphology (compare cellulose aerogels obtained by dissolution in ionic liquid (Figure 2) and in NaOH-water (Figure 3)). For example, for cellulose II aerogels made by dissolution in ionic liquid, the scaling exponent in Equation (1) is around 4<sup>[45]</sup> (Figure 5a) while if averaging data from different publications on cellulose II aerogels  $m \approx 2$ <sup>[44]</sup>, for k-carrageenan aerogels  $m \approx 1.8$ .<sup>[46]</sup> Figure 5b illustrates the cases of aerogels from different polysaccharide sources.<sup>[24]</sup> The reason of these differences is different network connectivity, pores size, and pore wall morphology (see, for example,<sup>[47]</sup>).

Low density, fine morphology, and high specific surface area make all types of aerogels very promising for various applications. One of the most remarkable properties of aerogels is their extremely low thermal conductivity, often lower than that of air in ambient conditions ( $0.025 \text{ W m}^{-1} \text{ K}^{-1}$ ), with the best values around  $0.012\text{--}0.015 \text{ W m}^{-1} \text{ K}^{-1}$ .<sup>[48,49]</sup> This is called thermal super-insulation, and aerogels are the only materials with such intrinsic property. The reason of such low conductivity is as follows. Thermal conductivity of a porous material is, roughly, the sum of solid, gas (here, air), and radiative conductions; the latter is usually low for optically thick materials. The conduction of the solid phase can be decreased by decreasing material density. To decrease the conduction of the air in the pores below  $0.025 \text{ W m}^{-1} \text{ K}^{-1}$ , their size must be lower than the mean free path of air molecule (66 nm); this is called Knudsen regime. Mesoporous low-density aerogels can thus possess thermal conductivity below that of air in ambient conditions. The leaders among thermal super-insulators are silica aerogels and

aerogel-like materials (so-called ambient pressure dried silica gels).<sup>[50]</sup> Their very low thermal conductivity is the main reason why silica aerogels and their composites are now produced at preindustrial scale, for example, for the construction sector. Several other types of aerogels, based on synthetic or natural polymers (resorcinol-formaldehyde,<sup>[51]</sup> polyimide,<sup>[21]</sup> pectin,<sup>[52,53]</sup> and nanofibrillated cellulose<sup>[54]</sup>), are also thermal super-insulating materials.

In addition to very low thermal conductivity, aerogels and their carbon counterparts (after aerogel pyrolysis) are suggested to be used for oil/water separation and filtration, drug release, energy storage, for adsorption, and as catalyst supports. Being highly porous and finely structured, aerogels are said to be promising materials for sound absorption; however, the studies of acoustic properties of aerogels are still scarce. A recent review summarized acoustic properties of silica aerogels only.<sup>[55]</sup> Below the acoustic properties of inorganic, synthetic, and biopolymer aerogels are overviewed based on published results.

#### 4. Acoustic Properties of Inorganic Aerogels and their Composites

Among all types of aerogels, silica aerogels are the most well studied. Some are among the lowest density solids ever made. Silica aerogels can be synthesized in the form of monoliths or granules (Figure 6a,b), with an internal morphology resembling pearl-necklace-like particle network (see Figure 6c,d).

The sound propagation in silica aerogels has been studied experimentally by various groups shown in Table 1. Gronauer et al.<sup>[56]</sup> and Gross et al.<sup>[57]</sup> established that the sound propagation in silica aerogels of densities above  $100 \text{ kg m}^{-3}$  is predominantly influenced by the elastic properties of the aerogel skeleton. They found that the sound velocity  $v_L$  in silica aerogels follows scaling behavior as a function of material bulk density  $\rho_{\text{bulk}}$

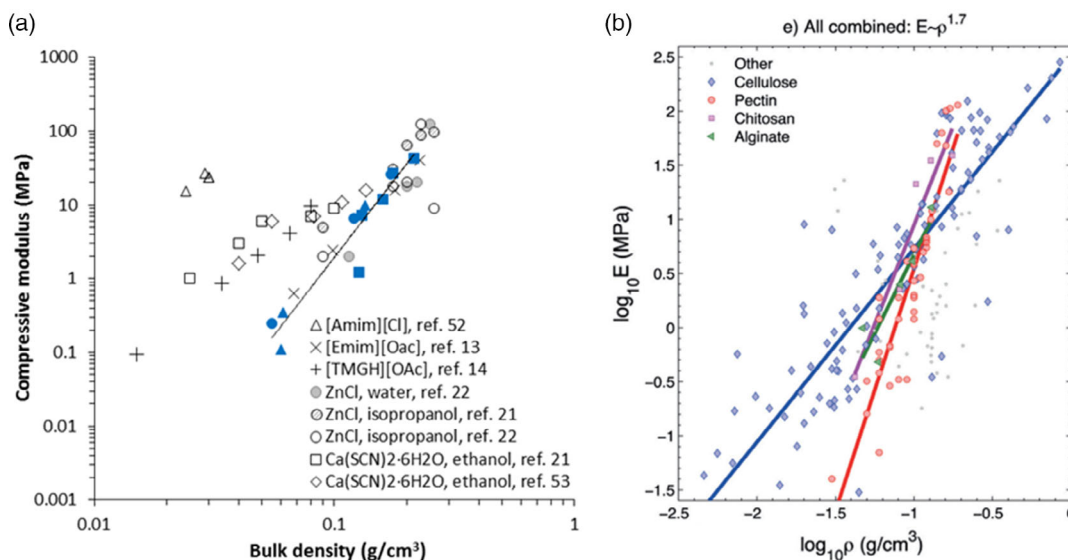


**Figure 5.** Modulus as a function of aerogel density: a) cellulose II aerogels made by cellulose dissolution in different solvents (solid line corresponds to the slope  $m = 4.2$  for cellulose dissolved in ionic liquid), for more details see,<sup>[45]</sup> reproduced from ref. [45] with permission from the Royal Society of Chemistry and b) various bio-based aerogels,<sup>[24]</sup> reproduced with permission from ref. [24] with permission from John Wiley and Sons.



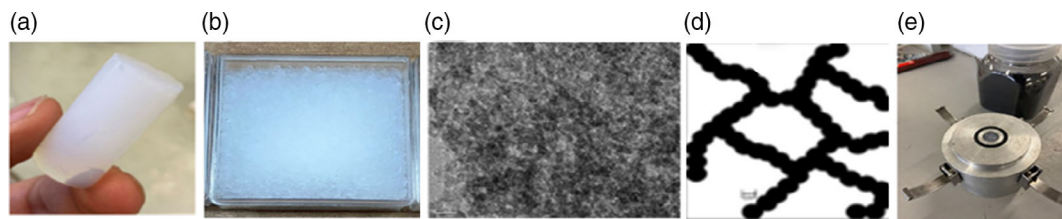


**Figure 6.** a) Monolithic silica aerogel, b) silica aerogels in granular form, c) TEM image of the aerogel, d) schematic presentation of silica aerogel structure, and e) impedance tube setup used by Begum et al.<sup>[68]</sup> (“Reprinted with permission.<sup>[68]</sup> Copyright 2021, Acoustic Society of America).

$$v_L \propto \rho_{\text{bulk}}^\alpha \quad (2)$$

where  $\alpha$  is the scaling exponent equal to 1.3 for silica aerogels of densities above  $100 \text{ kg m}^{-3}$  and to 0.8 for those with lower densities (Figure 7a). This scaling is similar to the other well-established density-dependent aerogel characteristics such as the mechanical properties as well as solid thermal conductivity. Taking into account Equation (1) that correlated mechanical properties and bulk density with exponent  $m$  and Equation (2), a relation between two exponents was derived:  $m = 2\alpha + 1$ .<sup>[58]</sup> Also, solid thermal conductivity scales density with an exponent  $t \approx 1.5$ .<sup>[59]</sup> Weigold and Reichenauer<sup>[60]</sup> established a correlation between the mechanical stiffness and solid thermal conductivity of silica aerogels and showed that the ratio,  $m/t \approx 2$ , which is generally observed in foams, also holds true for silica aerogels.

One must be very careful in using Equation (2) in the case of aerogels with densities below  $40\text{--}50 \text{ kg m}^{-3}$ : for silica aerogels in vacuum the correlation holds well, but for “nonevacuated” specimens, this relation is no longer valid.<sup>[61]</sup> For nonevacuated aerogels with density approximately below  $50 \text{ kg m}^{-3}$ , the air in the pores plays a dominant role in the sound propagation. Thus, Equation (2) for the sound wave propagation in gas-filled aerogels<sup>[41]</sup> was modified by Gross et al.<sup>[57]</sup> as follows

$$v_L = [(E + \chi p_g \Phi) / (\rho + \Phi p_g)]^{1/2} \quad (3)$$

where  $E$  is the Young’s modulus,  $p_g$  is the gas pressure,  $\Phi$  is the porosity,  $\rho$  is the bulk density, and

$$\chi = 1 + (\kappa - 1)[1 + c_v \rho / (c_{v,g} \rho_g \Phi)]^{-1} \quad (4)$$

Finally, the sound velocity in aerogels as a function of density and of the gas pressure can be well approximated by Equation (2) and (3) (see Figure 7b).

Gibiat et al.<sup>[62]</sup> investigated the acoustic performance of silica aerogels in two disconnected frequency ranges, namely, low ultrasonic (20–200 kHz) and low audible (20–2500 Hz). Velocity measurements in silica aerogels under low ultrasonic frequencies showed that the low-density aerogels exhibited unexpected attenuation for well-defined frequency bands. These results could neither be explained by the homogeneous propagation hypothesis nor by the Biot theory. However, they found a correlation between the attenuation bands in which the samples presented an unexpected high attenuation and the density of the silica aerogels. Measurements in the audible regime, based on impedance testing, showed that the results

strongly depend on the geometry and the boundary conditions imposed on the specimens.

Conroy et al.<sup>[63]</sup> studied the longitudinal sound velocity in silica aerogels as a function of the interstitial gas type and pressure. They showed that the energy transferred from the gas to the solid phase is lost to the sound propagation, resulting in slowing the sound velocity through the aerogel. Measurements of the sound velocity were made using three interstitial gases: helium, nitrogen, and argon. The rate of increase of acoustic velocity with pressure was found to be the highest in the gases with the higher sound velocity of the free gas, i.e., in helium, followed by nitrogen and then closely by argon. The sound wave propagation in aerogels was modeled using the Wood equation, wherein the bulk modulus of the gaseous state was examined using three approaches. The first one, as used by Gross et al.,<sup>[57]</sup> assumed an independent isothermal gas compression with no heating of the solid component. The second approach assumed standard adiabatic compression. This corresponds to the limiting case of no heat exchange between the two components. In the third approach, the heat exchange between the two component phases was accounted and occurred instantaneously and the temperature of both phases changed synchronously. The isothermal models consistently underestimated the acoustic velocity, while the adiabatic model overestimated it. Nevertheless, the third approach showed the best agreement with the experimental data for all interstitial gases studied. The sound velocity measurements in all cases at pressure up to 10 MPa displayed the loss of acoustic energy by the gaseous component.

Forest et al.<sup>[64]</sup> were among the first to investigate the acoustic properties of silica aerogel granules. In their study, they used two granule sizes, viz., 80  $\mu\text{m}$  and 3.5 mm. They measured the reflection coefficient, attenuation, and sound velocity of the granular aerogels under a frequency range of 20–2500 Hz and compared with the results for glass wool. They found that acoustic transmission losses in silica aerogels were at least 10 dB higher than those from glass wool of the same thickness. To show the optimal performance, they used a two-thickness method developed by Smith and Parrott<sup>[65]</sup> and measured the characteristic impedance and the propagation constant. This approach is reliable and useful except when the reflection coefficient or absorption is too high. In the latter cases, direct sound velocity measurements by means of an impedance tube method are preferred. Accordingly, an impedance tube with a diameter of 15 mm was used. They demonstrated that the larger aerogel granules possess lower reflection under 500 Hz, while the smaller granules have a significantly high attenuation. Thus, they proposed a multilayer stacked system, namely, the first layer, 1 cm thick,

**Table 1.** Acoustic properties of silica aerogels, their granular beads, blankets, and composites. SA: silica aerogel; SoAb: sound absorption, TL: transmission loss,  $\nu_s$ : sound velocity,  $\rho$ : bulk density.

Authors	Aerogel system	Density range [kg m <sup>-3</sup> ]	Specific surface area [m <sup>2</sup> g <sup>-1</sup> ]	Specimen type	Specimen thickness [mm]	Granule size [mm]	Testing method	Frequency range	Properties measured	Temperature [K]
Gibiat et al. 1995 <sup>[62]</sup>	SA	90–400		Monolith	10		Impedance tube	20–200 kHz, 20–2500 Hz	SoAb	
Conroy et al. 1999 <sup>[63]</sup>	SA	71		Monolith	6		Signal processing	1–10 GHz	$\nu_s$ , SoAb	300
Caponi et al. 2003 <sup>[119]</sup>	SA	510–2200	210–565	Monolith			Brillouin scattering		$\nu_s$ versus $\rho$ , mean pore-width	300
Daughton et al. 2003 <sup>[74]</sup>	SA	45–267		Monolith	22.8–31.5		Acoustic resonator		$\nu_s$ , damping versus T	0.4–400 K
Merli et al. 2018 <sup>[71]</sup>	SA	93–121		Monolith	12.7–25.4		Impedance tube	100–5000 Hz	SoAb, TL	
Li et al. 2019 <sup>[120]</sup>	SA	53–70	457–648	Monolith	11.8–25.4		Impedance tube	500–5000 Hz	SoAb, TL	
Forest et al. 2001 <sup>[64]</sup>	SA			Granules		0.08, 3.5	Impedance tube	20–2500 Hz	Reflection, attenuation $\nu_s$	
Cotana et al. 2014 <sup>[83]</sup>	SA			Granules		0.07–4.00				
Moretti et al. 2017 <sup>[121]</sup>	SA	65–85		Granules		0.01–4.00	Impedance tube	50–6400 Hz	TL	
Buratti et al. 2017 <sup>[67]</sup>	SA, aerogel-based plaster	65–85		Granules	15–40	0.01–1.20, 1.2–4.0	Impedance tube	100–6400 Hz	SoAb, TL	
Begum et al. 2021 <sup>[68]</sup>	SA	130–227	885–946	Granules			Impedance tube	300–3000 Hz	SoAb, Reflection	293 K
Gronauer et al. 1986 <sup>[56]</sup>	SA	71–285		Tiles, pellets	200	7	Signal processing	0.1–1 MHz	$\nu_s$ versus $\rho$	
Gross et al. 1992 <sup>[58]</sup>	SA	50–2200		Monolith, pellets			Signal processing	1–5 MHz	$\nu_s$ versus $\rho$	
Jichao et al. 2010 <sup>[72]</sup>	SA	80		Monolith, granules			Signal processing, impedance tube	10–200 kHz	$\nu_s$ versus $\rho$ , Attenuation, SoAb	
Oh et al. 2009 <sup>[77]</sup>	SA/PET blanket	37–184		Blanket			Impedance tube	200–6000 Hz	SoAb	
Venkatraman et al. 2014 <sup>[122]</sup>	SA/embedded nonwoven fabric	66–81		Blanket	3.5–6.6		Impedance tube	60–6400 Hz	SoAb, NR	
Eskandari et al. 2017 <sup>[81]</sup>	SA/UPVC	1150–1450	447–764	Composite sheets	1		Impedance tube	10–6400 Hz	SoAb, TL	
Ramamoorthy et al. 2018 <sup>[78]</sup>	SA/nonwoven PET	75–158		Blanket	4.9–5.5		Impedance tube	50–6300 Hz	SoAb	
Yang et al. 2018 <sup>[123]</sup>	SA/polyester/polyethylene	silica 135, fabrics 67–80		Blanket	3.5–6.6	0.1–0.7	Impedance tube (ASTM E 1050)	0–6500 Hz	Absorption coefficient	
Talebi et al. 2019 <sup>[76]</sup>	SA/polyester	210–390	782–977	Blanket	2.58–6.29		Impedance tube	50–6100 Hz	SoAb, NR	293 K
Begum and Horoshenkov 2021 <sup>[79]</sup>	SA/fiberglass			Blanket	7–11		Impedance tube	300–3000 Hz	SoAb, Reflection	

**Table 1.** Continued.

Authors	Aerogel system	Density range [kg m <sup>-3</sup> ]	Specific surface area [m <sup>2</sup> g <sup>-1</sup> ]	Specimen type	Specimen thickness [mm]	Granule size [mm]	Testing method	Frequency range	Properties measured	Temperature [K]
Yan et al. 2014 <sup>[124]</sup>	Silica cross-linked with polyimide	90–172	463–582	Monolith	1.6		Impedance tube	2.5–10 kHz	SoAb	
Hamidi et al. 2021 <sup>[125]</sup>	SA nanocomposite <sup>a)</sup>		28–183	Monolith	20			80–6300 Hz	SoAb, TL	

<sup>a)</sup>Four composites were studied here: SA/polyester nonwoven layer nanocomposite, SA/pan nanofibers nanocomposite, SA/nanoclay nanocomposite, SA/polyester nonwoven layer/pan nanofibers/nanoclay nanocomposite.

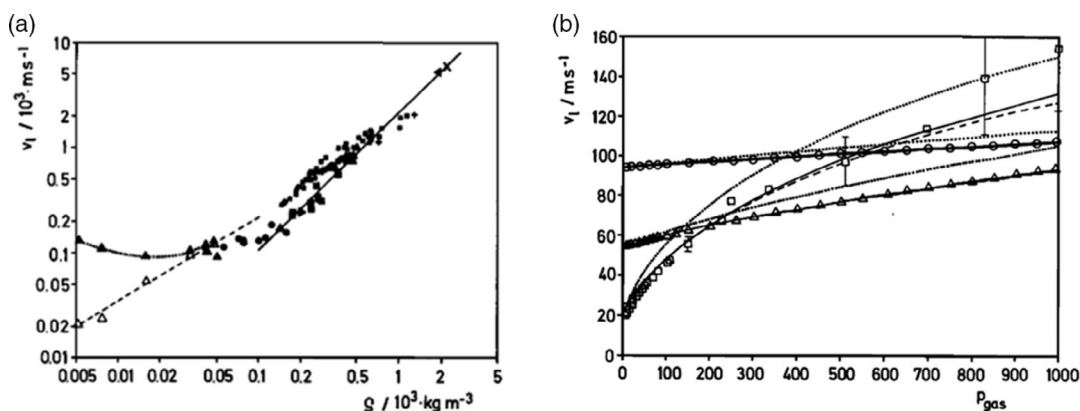


**Figure 7.** a) Illustration of power law correlation between the sound velocity and bulk density of silica aerogel. For densities above  $100 \text{ kg m}^{-3}$ , an exponent of 1.3 was found. For lower densities, it is 0.8. Here  $x$  = vitreous silica,  $\blacktriangleleft$  = opal,  $+$  = xerogels for drying purposes,  $\bullet$  = aerogels from DESY, Hamburg,  $\blacksquare$  = aerogels from Airglass, Staffanstorp,  $\blacktriangle$  = aerogels from LLNL, Livermore,  $\blacktriangleright$  = aerogel pellets from BASF, Ludwigshafen,  $\blacksquare$  = sintered silica aerogels. Data on evacuated aerogel specimens are shown with  $\Delta$ , b) sound velocity as a function of gas pressure for exceptionally low-density aerogels 5 ( $\square$ ), 16 ( $\Delta$ ), and 32 ( $\circ$ )  $\text{kg m}^{-3}$ .<sup>[61]</sup> Reprinted with permission.<sup>[61]</sup> Copyright 2004, Acoustic Society of America.

made of the large granules, and a second layer, 3 cm thick, made of the smaller ones. The first layer acted as an impedance matcher while the second one as an efficient absorber. Such a multilayer setup was also explored by Ricciardi et al.,<sup>[66]</sup> who developed a three-layer absorber system, where the first two layers acted as impedance matchers while the third layer acts as an absorber. The best attenuation was obtained in the case where the three layers were designed having granules of decreasing sizes (a 2 cm layer of granules of diameter 3 mm, followed by another 2 cm layer of granules with diameter 1 mm, and the last 2 cm layer of granules having a diameter of 80  $\mu\text{m}$ ).

Buratti et al. also studied the influence of granule size on the acoustic properties of silica aerogels.<sup>[67]</sup> Granule sizes ranged from 0.01 to 4 mm. A conventional impedance tube was used to measure the absorption coefficient and transmission loss. Five different specimen thicknesses were chosen: 15, 20, 25, 30, and 40 mm. It was demonstrated that the materials with smaller granule sizes, having higher density, had better acoustic insulation performance. **Figure 8a** shows that the smaller granule sizes (S and M) achieved the absorption coefficient of 1 at 3200 Hz and transmission losses of 7 dB were achieved at 1700 Hz. The results shown in **Figure 8a,b** correspond to the performance of different granule sizes for 15 mm thick specimens.

The authors also compared the performance of the aerogels with state-of-the-art insulation materials from the market, rock wool, and basalt fiber. A combined peak performance was achieved by aerogels with the smallest granule sizes (S), which demonstrated an absorption coefficient higher than 0.9 and transmission losses of 15 dB at 1700 Hz (see **Figure 8c,d**). For low-frequency ranges (below 2000 Hz), aerogel-based samples outperform rock wool and basalt fiber considering absorption coefficient and transmission losses. Since the study was motivated by energy saving in building applications, the authors also confirmed their laboratory results by using two plaster-aerogel composites for building. The peak of the absorption coefficient of these materials was 0.29 at 1050 Hz, compared to 0.1 for conventional plasters. Simultaneously, the thermal conductivity of the plaster decreased from 0.7 to 0.05  $\text{W m}^{-1}\text{K}^{-1}$ . In the best case, using smaller granules resulted in a transmission loss of 17 dB at 1700 Hz for the 40 mm thick panel, while with larger granules the loss was 6–7 dB.

The influence of silica sol concentration, and, as a consequence, of aerogel density, was studied by Begum et al.<sup>[68]</sup> using 10 mm diameter impedance tube setup. Silica aerogels were prepared with different polyethoxydisiloxane content in the sol. To enable ambient pressure drying, hydrophobization treatment

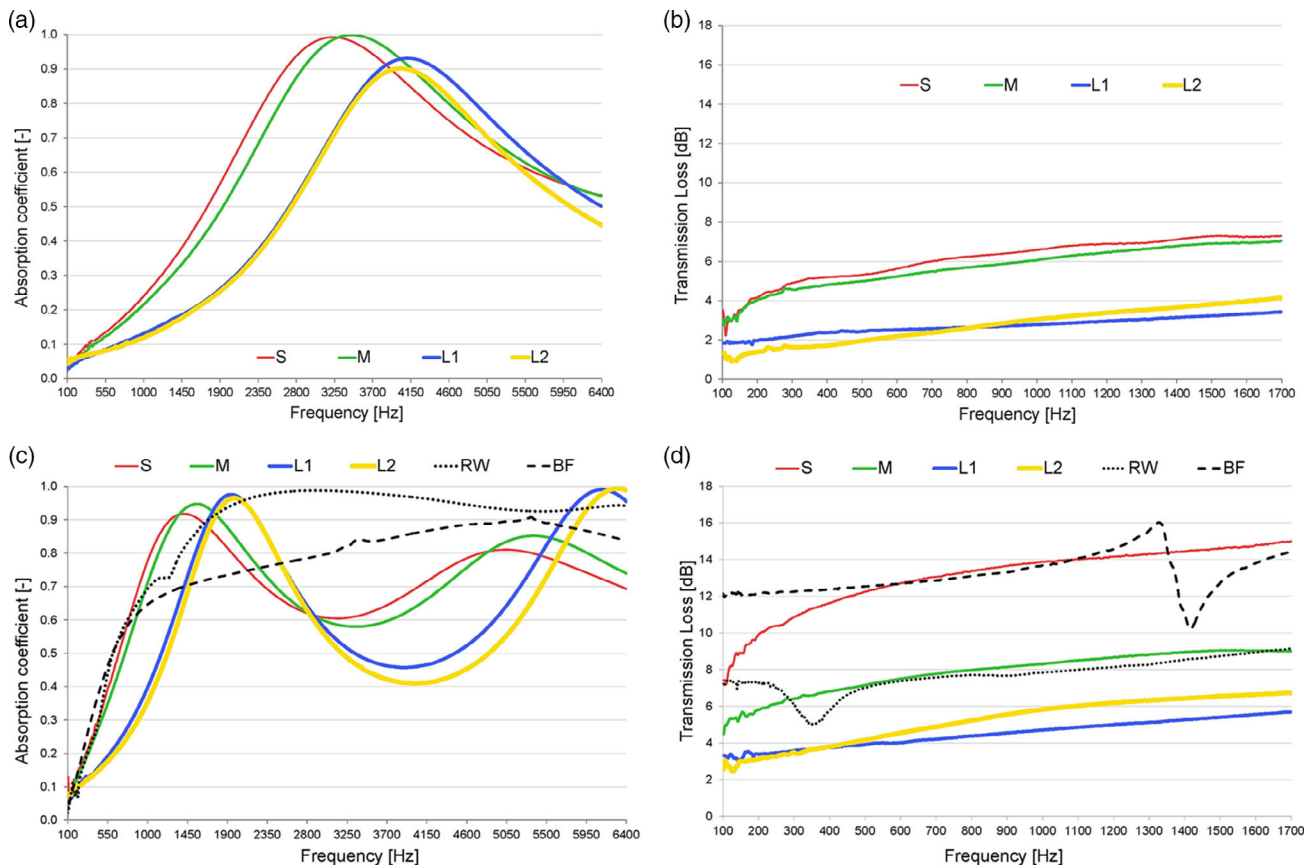


**Figure 8.** Influence of granule size on the acoustic properties of silica aerogels: a) effect of silica aerogel granule sizes in the granular bed on the absorption coefficient and b) transmission loss; c) comparison between the aerogel samples, rock wool (30 mm), and basalt fiber (27 mm) for their acoustic absorption and d) transmission loss. S: 0.01–1.20 mm, M: 0.7–2.0 mm, L1: 0.7–4.0 mm, L2: 1.2–4.0 mm, RW: rock wool, and BF: basalt fiber.<sup>[67]</sup> (Reprinted from.<sup>[67]</sup> Copyright 2017, with permission from Elsevier).

was carried out. The thickness of each specimen was maintained at 50 mm, since the impedance tube was designed to deposit granular samples through a 10 mm wide and 50 mm deep sample holder. The aerogels with higher density demonstrated, generally, better absorption characteristics. For all cases, the first destructive interference maximum was observed in the low-frequency range, around 1000 Hz. This was shown to be an effect of the relative decrease in the sound speed in the aerogel caused by an increase in dynamic compressibility of the air in the inner-particle pores. As seen from **Figure 9**, the aerogel with the highest density and also the smallest pore-width (obtained with BJH approach) had the most pronounced effect. This demonstrates the effect of the micropores. Beyond the interference maximum, the absorption coefficient was shown to depend less on the compressibility of the air in the material's pores but more on the viscous permeability of the aerogels. To explain these results, the authors used the inverse model proposed by Venegas et al.<sup>[69]</sup> The model considered hierarchical porosity and explained the dissipation of sound in the bed of granular silica aerogels due to viscous and thermal effects in the voids, rarefied gas flow and heat transfer in the inner-particle macropores, hierarchical pressure, and mass diffusion. It was also

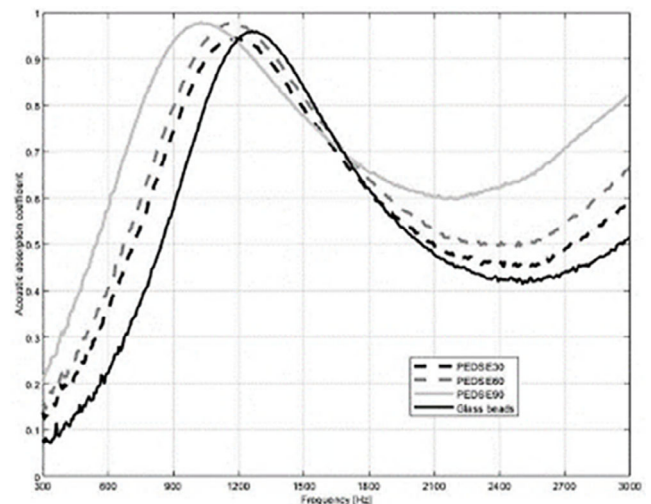


**Figure 9.** Effect of silica aerogel density on the acoustic absorption properties of granular beds; glass beads are shown for comparison.<sup>[77]</sup> (Reprinted with permission.<sup>[68]</sup> Copyright 2021, Acoustic Society of America). Here, PEDSE 30, E60, and E90 correspond to aerogels with bulk densities 0.130, 0.163, and 0.227 g cm<sup>-3</sup>, respectively.



shown that the acoustic absorption significantly increases due to the presence of the pores smaller than that of the mean-free path of the air molecule. This study, together with the one by Abawi et al.,<sup>[70]</sup> has reopened the discussion for a need in advancing the theoretical understanding and modeling for predicting and interpreting the acoustic properties of granular aerogels.

It is interesting to compare the acoustic performance of monolithic and granular aerogels. Merli et al.<sup>[71]</sup> investigated the acoustic performance of monolithic silica aerogels by means of the impedance tube method. They found that the sound absorption coefficient decreased with increasing thickness of the specimens. Among the three specimen thicknesses studied (12.7, 19.1, and 25.4 mm), peak absorption was observed in the case of the 12.7 mm specimen, having a coefficient of 0.88 at a frequency of 1500 Hz. The transmission loss was found to increase with increasing thickness. Monolithic aerogel glazing systems showed highest transmission losses, compared to granular ones, particularly in the 200–1000 Hz range (see **Figure 10**).<sup>[71]</sup> The sound insulation index improved by 3 dB when using monolithic aerogel system, while by 1–2 dB when using a granular system. Jichao et al.<sup>[72]</sup> also presented a comparative study of monolithic and granular silica aerogels. They showed that density, elasticity, air pressure, temperature, and pore sizes are key parameters in determining the sound velocity in silica aerogels. They also echoed the results of Gibiat et al.<sup>[62]</sup> after observing the unexpected attenuation. They also claimed

that silica aerogels revealed the lowest acoustic impedance among all solid materials.

Temperature may be an important factor to consider for acoustic properties, in particular, in construction applications. Xie and Beamish<sup>[73]</sup> observed a steep drop in sound speed of dense (290 and 360 kg m<sup>-3</sup>) silica aerogel samples with increasing temperature. This was attributed to a thermally activated relaxation process. Longitudinal and transverse modes showed similar influences on their velocities, indicating that the Poisson ratio remains constant around 0.22. Daughton et al.<sup>[74]</sup> used acoustic resonance spectroscopy to study low-frequency elastic properties of silica aerogels of density 45–267 kg m<sup>-3</sup> over a temperature range of 0.4–400 K. The elastic modulus was found to drop dramatically between 20 and 100 K and was accompanied by a damping peak. This was attributed to a thermally activated relaxation process. At higher temperatures, the elastic modulus increased linearly with temperature. This was strongly resembling the effect observed in elastomers and rubbers, where there is a significant entropic contribution to the stiffness of the material.

Several authors have recently studied the acoustic performance of silica aerogel blankets, i.e., aerogel particles “hold together” by a nonwoven mat. This is a cost-effective approach for scaled-up applications including sound absorption and insulation where manufacturing of large panels is needed.<sup>[75]</sup> It was demonstrated that aerogel blankets exhibit higher sound

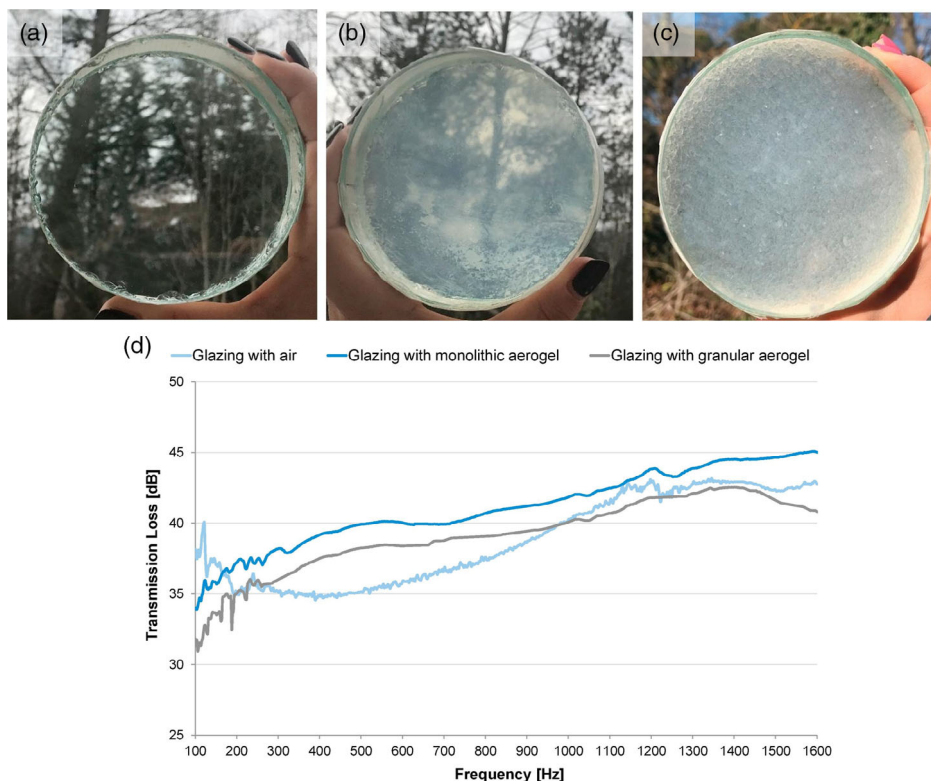


**Figure 10.** Images of specimens for glazing systems with a) air, b) monolithic aerogel, and c) granular aerogel; d) comparison of transmission losses in glazing systems without aerogels (air glazing), and with monolithic and granular aerogels.<sup>[71]</sup> (Reprinted from.<sup>[71]</sup> Copyright 2018, with permission from Elsevier).



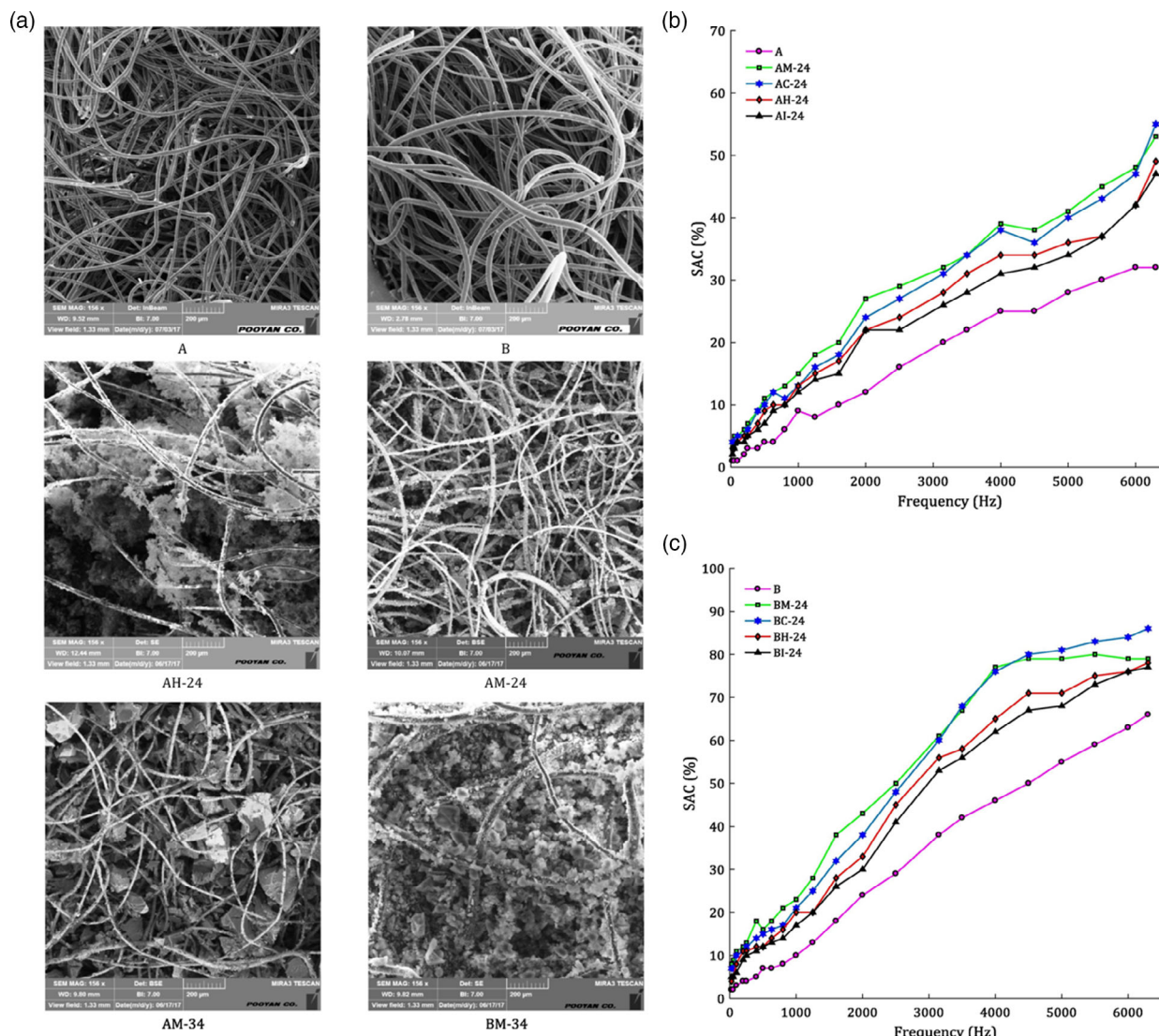


**Figure 11.** a) SEM images of the microstructure of neat nonwoven PET fabric: “A” fiber diameter of  $17.60\ \mu\text{m}$  and surface density of  $206\ \text{g m}^{-2}$ , “B” fiber diameter of  $29.45\ \mu\text{m}$  and surface density of  $834\ \text{g m}^{-2}$  and the corresponding aerogel-reinforced blankets AH, AM, and BM; b,c) effect of silica aerogels on sound absorption coefficient of the aerogel/polyester blankets. All AX-24 and BX-24 samples represent aerogel blankets with different densities and synthesis conditions. Details of synthesis conditions can be found in Table 2 of ref. [80]. (Reprinted from,<sup>[76]</sup> Copyright 2019, with permission from Elsevier). The reported bulk densities of the silica aerogels in BM, BC, BH, and BI are  $0.21\ \text{g cm}^{-3}$ ,  $0.24\ \text{g cm}^{-3}$ ,  $0.33\ \text{g cm}^{-3}$ , and  $0.39\ \text{g cm}^{-3}$ , respectively.

absorption coefficient than the neat nonwoven samples, here, based on polyethylene terephthalate (PET), see Figure 11.<sup>[76]</sup> Blankets with lower bulk densities, larger pore sizes, and higher porosities resulted in better acoustic absorption (Figure 11). The acoustic performance was found to be controlled by the (mean) pore sizes in aerogels and the porosity of the aerogels. Hydrophobic blankets performed better compared to the hydrophilic ones. Other studies on silica aerogel/PET blankets also showed the improved sound absorption.<sup>[77,78]</sup> The same conclusion was made for silica aerogel blankets with fiberglass:<sup>[79]</sup> the sound absorption coefficient increased for silica aerogel particle filling ratio from 0 to 50%. At 75% filling ratio and beyond, the increase in the sound absorption coefficient was less

pronounced. This makes sense as the effective porosity strongly decreased. All tests were done with a 10 mm diameter impedance tube. To predict the acoustic properties of the fiberglass blankets, a refined Biot model was used that considered the sorption and pressure diffusion effects.<sup>[80]</sup>

Silica aerogel/unplasticized polyvinyl chloride (UPVC) composites were studied in the view of their acoustic performance in window profiles and drainage pipes.<sup>[81]</sup> All tests were done by the impedance tube method with specimens having diameters of 29 mm under a frequency range of 63–6300 Hz. Pure UPVC demonstrates a maximum sound absorption of 17%, which is very low. With the addition of 0.5, 1.5, and 3.0 wt% of silica aerogel to UPVC, the sound absorption increased to 24, 28%, and

43%, respectively. As sound waves struck the specimens and explored the pores, the complexity of paths that the sound wave passes increased in the presence of aerogel particles. Viscous stresses caused by shearing and friction of air across the pores of silica aerogels increases leading to an increase in sound absorption. The smaller and more homogeneous the pores, the higher the energy absorption occurs through vibration. Low density of the aerogel composites slowed the propagation of sound waves and increased acoustic absorption. The stiffness and density were shown to affect sound reflection. At low frequencies, the stiffer the aerogel, the higher was the transmission loss. At higher frequency, density was the dominant factor. For building and construction applications, since the low-frequency noise is recognized as an environmental problem, silica aerogel/UPVC composites were shown to be good candidates for window profiles. Many other studies have investigated the use of silica aerogels and their composites in application to the building and construction industry.<sup>[71,77,82,83]</sup>

Different theoretical descriptions of sound propagation in silica aerogels have been developed, but they are still far from being complete. One could use the Wood equation<sup>[84]</sup> to predict the compressional sound wave speed in aerogels,  $v_L$  as follows

$$v_L = \left[ (\varphi_s \rho_s + \varphi_g \rho_g) \left( \frac{\varphi_s}{\mu_s} + \frac{\varphi_g}{\mu_g} \right) \right]^{-1/2} \quad (5)$$

where  $\varphi$ ,  $\rho$ , and  $\mu$  represent the volume fractions, material's density, and bulk modulus in the solid "s" and gaseous "g" phases, respectively. Modified versions of this equation were shown to adequately describe the dependence of sound velocity on the pressure of the interstitial gases in extremely low-density aerogels (below  $50 \text{ kg m}^{-3}$ ).<sup>[57]</sup> Continuum approaches that consider coupling two component phases, such as Biot theory<sup>[85,86]</sup> and dynamic tortuosity approach of Johnson et al.,<sup>[87]</sup> were tested to describe the acoustic properties in silica aerogels. Biot model considers the problem of sound propagation in a porous elastic solid saturated by a viscous fluid (here, air) by deriving the equations for sound waves through the solid and "fluid" fractions. Johnson model is discussed later in this section.

The air molecules in the interstitial nanoporous network of silica aerogels are more likely to collide with the solid skeletal walls of the pores than with other gas molecules. This is because silica aerogels are mesoporous, with pore sizes smaller than the mean free path of air molecule at ambient pressure (few tens of nm vs 66 nm, respectively). Thus, the theories developed for highly macroporous materials do not work for silica aerogels. The model needs to bear a closer resemblance to vacuum systems than to those typically used to describe standard porous media. This is because the microscopic response to sound propagation of the solid phase and gaseous phase in a porous material is different as compared to aerogels. Under typical conditions, the temperature swings in a gas are of the order of 0.01 K. These are much smaller in the solid phase, suggesting lower adiabatic compressibility. Within a silica aerogel, this difference in the thermal response results in temperature gradients within the scale of the pores' size. The heat transfer between components resulting from these microscopic temperature gradients

influences bulk acoustic properties. The solid phase in aerogels acts analogous to the nontranslational states of a polyatomic gas, while the gaseous phase is analogous to the translational ones. During the propagation of sound waves, the energy transferred from the gaseous phase to the solid skeleton is lost for the propagation in the gaseous phase. This results in an increased absorption of the acoustic pulse and a decreased sound velocity in aerogels.

To predict the sound absorption coefficient in silica aerogels, the Johnson–Champoux–Allard (JCA) model<sup>[87–89]</sup> was shown to work well. JCA is a semi-phenomenological model that provides the sound absorption coefficient for uniformly- and nonuniformly nanoporous materials, assuming straight and cylindrical pores. While the pore space in aerogels is random and far from having a uniform straight cylindrical appearance, the assumption of cylindrical pores is accepted in the aerogel community and is used for calculating the pore-size distribution within the Barrett–Joyner–Halenda theory,<sup>[90]</sup> which is based on the Kelvin equation. The validity of cylindrical pores as an assumption has been debated in other works and will not be addressed in this paper.

The JCA model requires five parameters, namely, porosity, flow resistivity, tortuosity, and the viscous and thermal characteristic lengths. The two latter account for the nonuniform structure of the aerogels. Abawi et al.<sup>[70]</sup> used an inverse characterization method, where the JCA model was used to map the sound absorption coefficient of silica aerogel granules as a function of the frequency. The theoretical results correlated well with experimental data for aerogel granules larger than 0.25 mm. The aerogels on which the inverse characterization was carried out were silica aerogel granules produced by Cabot Corporation and had densities ranging from 60 to 90  $\text{kg m}^{-3}$ . The details of the parameter study can be found in ref. [64] For granules smaller than 0.25 mm, the results only showed a qualitative convergence in the absorption curves due to ill-fitting of the pore shape parameters in the equations for the thermal and viscous characteristic lengths. The results from<sup>[64]</sup> were further applied to study the sound proofing characteristics of silica aerogel granules in application to aircraft cabins.<sup>[91]</sup> This application was motivated by the fact that current state-of-the-art insulation solutions, e.g., glass wool, do not provide significant sound absorption at low frequencies. The JCA-model was used in the simulation-based study, and the results were then compared to the case of insulation with glass wool. The sound proofing was found to be much more efficient in the aerogel case, in particular, in the low-frequency region (100–200 Hz), which is, in general, challenging.<sup>[91]</sup>

It should be noted that the JCA model neglects the thermal effects at low frequencies. To overcome this drawback, the extensions of the JCA model using the Johnson–Champoux–Allard–Lafarge (JCAL) theory<sup>[92]</sup> account for the correction to the bulk modulus thermal behavior at low frequencies. The Johnson–Champoux–Allard–Pride–Lafarge (JCAPL) model<sup>[93]</sup> additionally considers the static viscous and thermal tortuosity. Both these parameters in the JCAPL model introduce low-frequency corrections to the JCA and JCAL models. For further optimization of the acoustic properties of aerogels, the advancement in the theoretical description of the sound propagation is necessary.

## 5. Acoustic Properties of Polymer Aerogels

Following the success of polymer-crosslinked hybrid silica aerogels and their embedded polymer composite forms to address the intrinsic fragility of silica aerogels, it was reasoned that a neat polymer aerogel with a self-assembly mechanism similar to crosslinked silica hybrid aerogel should also have enhanced properties in terms of mechanical integrity as well as ductility. Thus, a new class of purely synthetic polymer aerogels has emerged. Those include aerogels based on different polymeric sources, such as polyurea,<sup>[25,36,94]</sup> polyurethane,<sup>[38,95,96]</sup> polyimide,<sup>[97–99]</sup> and polyamide,<sup>[20]</sup> among many others. Owing to the unique combination of excellent properties such as low thermal conductivity, low dielectric constant, and a high-degree of flexibility, polymer aerogels have been considered a novel advanced material with high commercialization potential and therefore recently attracted research attention for vibro-acoustic mitigation applications.<sup>[32]</sup>

Yao et al. reported the first acoustic characterization of a phenolic aerogel material system that was prepared by freeze-drying method.<sup>[100]</sup> They studied a sandwich microstructural material system comprised of three layers whereby the top and bottom layers exhibited a pyknotic structure, and the middle layer

exhibited irregularly dispersed nanopores. It was referred to as an open-pore phenolic cryogel acoustic multistructured plate (OCMP). Using an acoustic impedance tube, the sound transmission loss and absorption coefficient of four OCMP samples at different solid content concentrations (10%, 15%, and 20% denoted by A1 to A3, respectively) against a cryogel plate sample with uniform -pore (with 20% solid content and denoted by B1) were studied (Figure 12).<sup>[100]</sup>

Significant improvement for the OCMP samples is seen in terms of sound transmission loss in comparison with that of the OCP sample. This improvement for sound absorption coefficient of the OCMP samples at low frequencies is attributed to the increase in the overall impedance of the multilayered microstructure compared to the uniform pore-sized sample. Although the bulk density of the OCMPs was not reported in this work, their high sound transmission loss makes them attractive for acoustic attenuation applications in building structures, vehicles, and aerospace fields.

With the high mechanical strength and exceptional energy absorption capability, polyurea aerogel is considered an attractive multifunctional material.<sup>[101]</sup> The commercially available aliphatic triisocyanate-based polyurea aerogels<sup>[101,102]</sup> have been studied for explosive shockwave absorption.<sup>[103,104]</sup> In the same

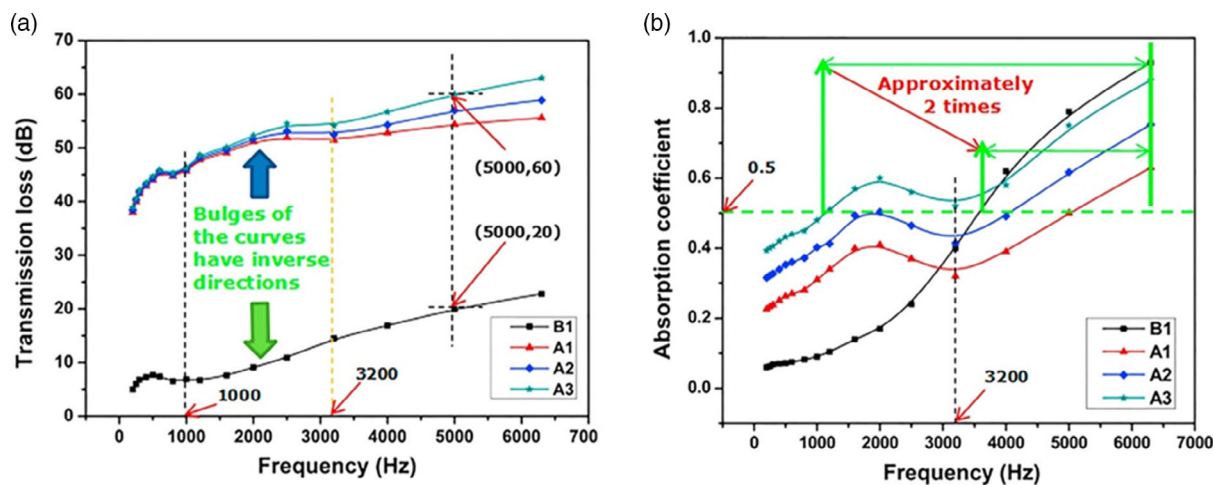


**Figure 12.** Sound transmission loss a) and absorption coefficient b) of open-pore phenolic cryogel acoustic multistructured plates (OCMPs) at different solid content concentrations (A1, 10%; A2, 15%; A3, 20%) and an open-pore cryogel plate (OCP) sample with uniform-pore (with 20% solid content and denoted by B1).<sup>[100]</sup> (Reprinted from:<sup>[100]</sup> Copyright 2016, with permission from Elsevier)

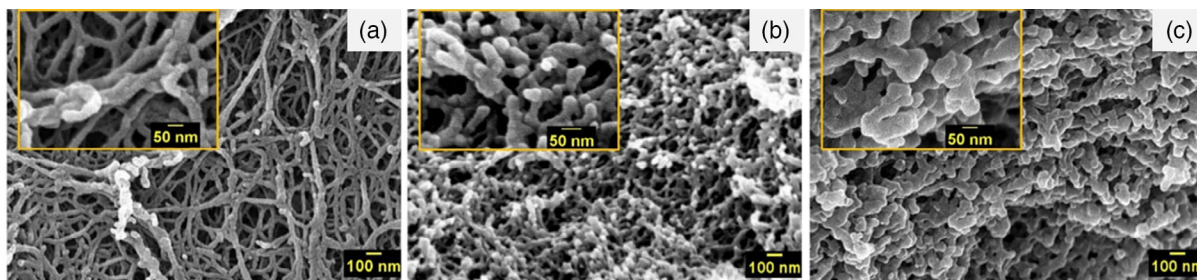


**Figure 13.** SEM micrographs of the polyurea aerogel samples at bulk densities of a) 0.11 g cm<sup>-3</sup>, b) 0.25 g cm<sup>-3</sup>, and c) 0.54 g cm<sup>-3</sup>.<sup>[25]</sup> (Reprinted from:<sup>[25]</sup> Copyright 2017, with permission from Elsevier).



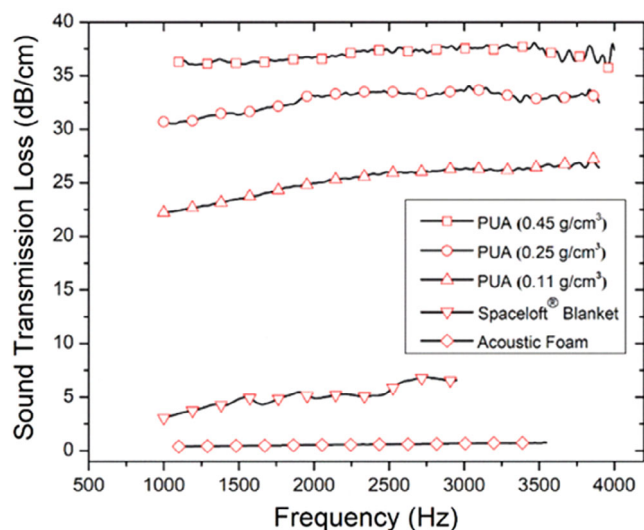


**Figure 14.** Normal incidence sound transmission loss of the polyurea aerogel samples at various bulk densities as well as an acoustic foam (polyurethane foam) and a commercially available silica aerogel (Spaceloft).<sup>[25]</sup> (Reprinted from.<sup>[25]</sup> Copyright 2017, with permission from Elsevier).

context, Malakooti et al. studied their normal incidence sound transmission loss behavior using an acoustic impedance tube<sup>[25]</sup> as well as their diffuse field sound transmission loss using the standard chamber-based diffuse sound field measurements.<sup>[105]</sup> For normal incidence sound transmission loss measurements, a three-microphone-based impedance tube was utilized and the sound transmission loss of the aerogels was measured at different frequencies up to 4 kHz.<sup>[25]</sup> **Figure 13** shows the SEM micrographs of the polyurea (PUA) aerogels at different bulk densities. The normal incidence sound transmission loss results of the PUA aerogels at three different bulk densities are shown in **Figure 14**. In this work, the wave propagation in aerogels was also modeled using the Biot's theory of dynamic poroelasticity.<sup>[25]</sup> For comparison, similar measurements were carried out on relevant materials such as a commercially available aerogel

(Spaceloft Blanket by Aspen Aerogels) made of a traditional silica aerogel monolith with embedded glasswool fibers through its bulk, as well as an acoustic polyurethane-based foam at similar densities. The polyurea aerogels at all densities exhibited higher sound transmission loss in comparison with the commercial samples.

Acoustic characterization under normal incidence condition (i.e., impedance tube-based measurements) is only a small part of our understanding of material's acoustic behavior. In order to fully characterize the acoustic properties of a material, relevant measurements should be carried out at a diffuse field condition. Standardized diffuse field sound transmission loss measurements require a large sample, typically 10 m<sup>2</sup> in size, as specified in ASTM standard E90-90,<sup>[106]</sup> which is similar to ISO 10 140.<sup>[107]</sup> To prepare aerogels of this dimension makes such a test a labor intensive and costly task. To date, there is only one E90 testing on a wall panel incorporating a polymer aerogel reported in open literature.<sup>[105]</sup> In this work, Malakooti et al. studied the PUA aerogels as a constraint damping in a sandwich structure with gypsum wallboards and the airborne sound insulation characteristics of the component have been measured. In these experiments, the sample is mounted at the opening of two adjacent reverberation rooms. A diffuse incident sound field is generated from one side and the radiated sound pressure levels from the sample into the other room are measured. The frequency range of their measurements was set to 100–5000 Hz. This study consisted of two sets of experiments for two different sample face areas of 1 and 10 m<sup>2</sup>. **Figure 15** shows the sample and the setup.

The diffuse field sound transmission loss of the two sample sets is shown in **Figure 16**. The effect of the polyurea aerogel layer on the sound transmission loss of the composite panel at both sizes is significant, especially at 4 kHz. The drop in sound transmission loss at 4 kHz is correlated to the lowest coincidence frequency of the panel. This improvement was achieved only with 20% increase in the overall mass of the composite panel that breaks the Mass Law in acoustics<sup>[108]</sup> for these gypsum/polyurea aerogel composite panels.

Recently, graphene oxide/polyvinyl alcohol hybrid aerogels (GPAs) were synthesized, and the effects of blend composition, sample thickness, and density on their acoustic properties were

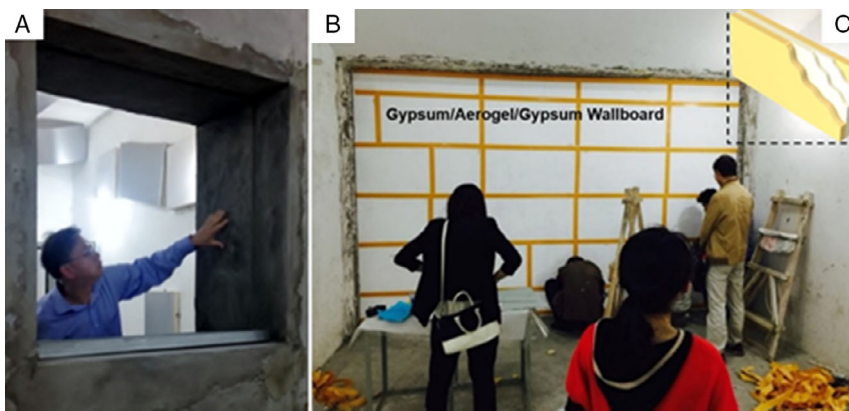


**Figure 15.** Diffuse field sound transmission loss setup preparations. A) View from the connecting window of the test chamber prepared for the 1 m<sup>2</sup> test specimen; B) view from the 10 m<sup>2</sup> aerogel layer; C) schematic for the final configuration of the composite wallboard including two gypsum skin layers accompanied with two core aerogel layers (shown in white).<sup>[105]</sup> (Reprinted with permission.<sup>[105]</sup> Copyright 2018, John Wiley and Sons).

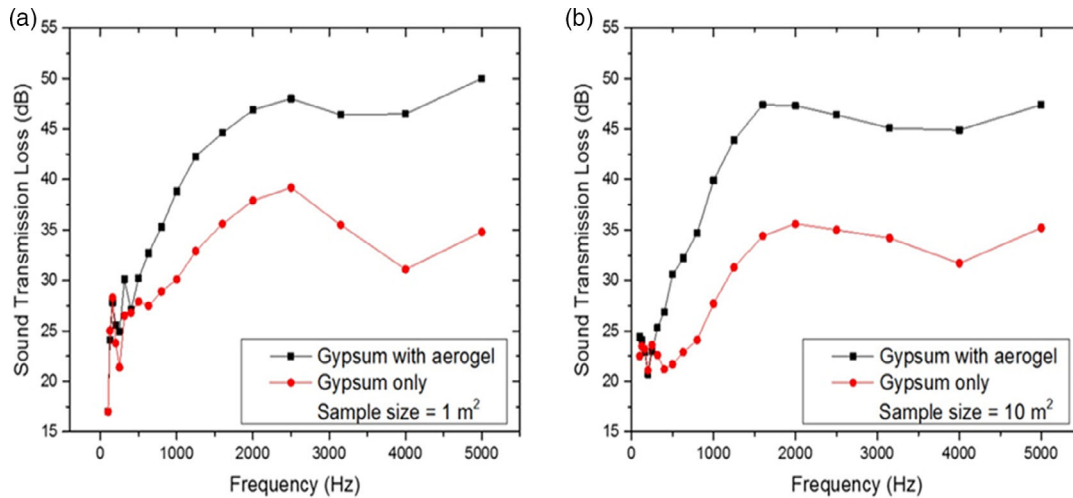


**Figure 16.** The diffuse field sound transmission loss of the polyurea aerogel composites. Data taken from ref. [105].

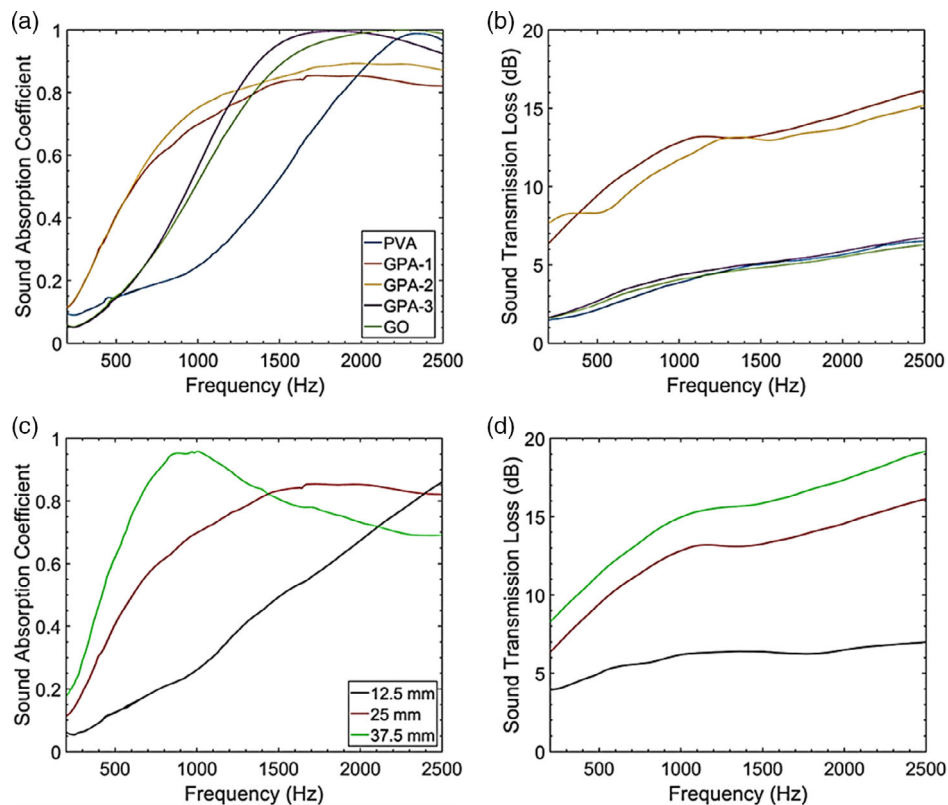


**Figure 17.** Sound absorption coefficient a,c) and sound transmission loss b,d) of the graphene oxide/polyvinyl alcohol hybrid aerogels at different blend composition (all with 25 mm thickness) and various sample thicknesses (results shown only for GPA-1 sample). Reproduced with permission.<sup>[109]</sup> Copyright 2021, The Authors, published by Springer Nature.

investigated.<sup>[109]</sup> Sound absorption coefficient and sound transmission loss were measured using an impedance tube. For these studies, six samples at different graphene oxide/polyvinyl alcohol (GO:PVA) weight ratios of 0:1, 1:1, 2:1, 3:1, and 1:0 denoted by

PVA, GPA-1, GPA-2, GPA-3, and GO were prepared. **Figure 17** shows the effect of blend composition and sample thickness on the sound absorption and transmission loss of the GPAs. The presence of PVA improves the low frequency (below 1200 Hz)



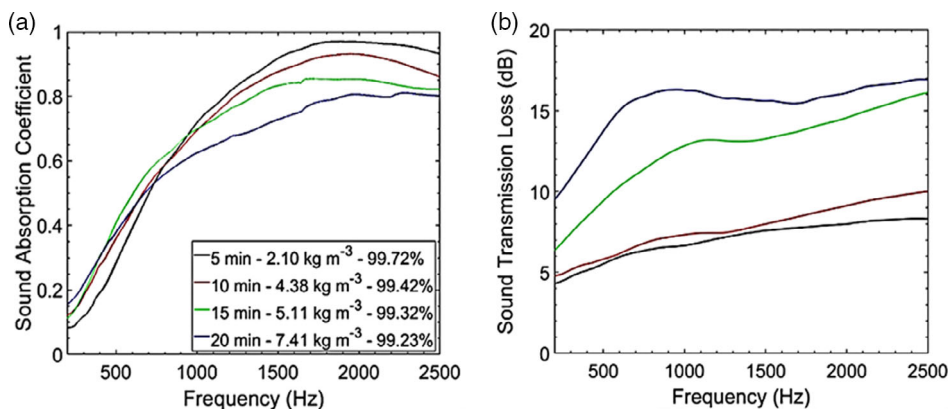


**Figure 18.** a) Sound absorption coefficient and b) sound transmission loss of the graphene oxide/polyvinyl alcohol hybrid aerogels (GPA-1 formulation) at different densities. The processing times for air entrapment during the blending process are also mentioned in the legend for sound absorption coefficients.<sup>[109]</sup>

sound absorption of the aerogels as the porosity of the GPAs increases with PVA and therefore flow resistivity declines. Moreover, the PVA also improves the sound transmission loss of the GPAs. Highest sound transmission loss (13.2 dB) was reported for GPA-1 (Figure 17). Thicker samples also showed improved sound absorption coefficients at low frequencies and higher sound transmission losses over the entire frequency range.<sup>[109]</sup>

**Figure 18** discloses the effect of density on the GPA-1's sound absorption and transmission loss behavior. As the density decreases, the sound absorption of the aerogels was slightly improved. However, sound transmission loss shows high sensitivity in terms of aerogel's density. In summary, these samples demonstrate superior acoustic properties while guaranteeing extremely low densities.

**Table 2** summarizes the polymer aerogel acoustics studies in terms of the aerogel samples' bulk density and average pore diameter, as well as their experimental configurations such as sample thickness, testing method, and frequency range.

**Table 2.** Summary of polymer aerogel acoustics studies: material properties and experimental configurations; SA: sound absorption, STL: sound transmission loss.

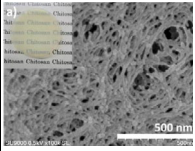
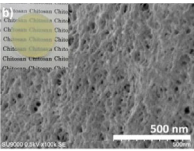
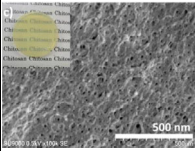
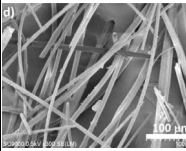
Author	Aerogel system	Aerogel density range [g cm <sup>-3</sup> ]	Pore diameter range [nm]	Specimen type	Specimen thickness [mm]	Testing method	Frequency range [Hz]	Measured acoustic properties
Yao et al. 2016 <sup>[100]</sup>	Phenolic cryogel	N/A	30–50	Monolith	N/A	Impedance tube <sup>a)</sup>	1000–3200	SA/normal incidence STL
Malakooti et al. 2017 <sup>[25]</sup>	Polyurea aerogel	0.11–0.45	40.33	Monolith	5	Three-microphone impedance tube <sup>[126]</sup>	1000–4000	Normal incidence STL
Malakooti et al. 2018 <sup>[105]</sup>	Gypsum/polyurea aerogel/gypsum	0.15, 0.25	40.33	Sandwich composite	30 <sup>d)</sup>	Diffuse sound field measurement <sup>b)</sup>	50–5000	Airborne STL
Rapisarda et al. 2021 <sup>[109]</sup>	Graphene oxide/polyvinyl alcohol aerogel	0.0051–0.0078	N/A	Monolith	12.5–37.5	Impedance tube <sup>a),c)</sup>	400–2500	SA/normal incidence STL

<sup>a)</sup>Based on ASTM E1050–12;<sup>[127]</sup> <sup>b)</sup>Based on ASTM E90–09 (2016);<sup>[106]</sup> <sup>c)</sup>Based on ASTM E2611–19;<sup>[128]</sup> <sup>d)</sup>The thickness of each polyurea aerogel panel was 5 mm.

## 6. Acoustic Properties of Bio-Aerogels

Very little is known about the acoustic properties of bio-aerogels. It should be noted that sometimes authors name “aerogel” the material with very large macropores without providing specific surface area. Such materials are usually obtained by freeze-drying and should be called “foams” or “cryogels” or simply “porous materials.” Below we show examples found in literature on the acoustic properties of bio-aerogels; few examples of some aerogel-like bio-based materials are given for comparison.

Chitosan aerogels were synthesized from formaldehyde-crosslinked chitosan and supercritically CO<sub>2</sub> dried.<sup>[110]</sup> When polymer concentration was varied from 5 to 10 g L<sup>-1</sup>, aerogel density increased from 0.060 to 0.157 g cm<sup>-3</sup>, respectively, and specific surface area was around 740–870 m<sup>2</sup> g<sup>-1</sup> without any notable dependence on chitosan concentration (**Figure 19**). The acoustic properties of aerogels, obtained with impedance tube Type 4206 (B&K) using a two-microphone transfer function method, are shown in **Figure 20**; glass wool was also tested for comparison.

Sample and chitosan concentration	S5 5 g/L	S7.5 7.5 g/L	S10 10 g/L	Glass wool
Morphology				
Thickness, mm	4.5	4.4	4.3	5.0
Density, g/cm <sup>3</sup>	0.060	0.122	0.157	0.064
Specific surface area, m <sup>2</sup> /g	793	872	737	

**Figure 19.** Main characteristics of chitosan aerogels.<sup>[110]</sup> (SEM images are reprinted from.<sup>[110]</sup> Copyright 2019, with permission from Elsevier).

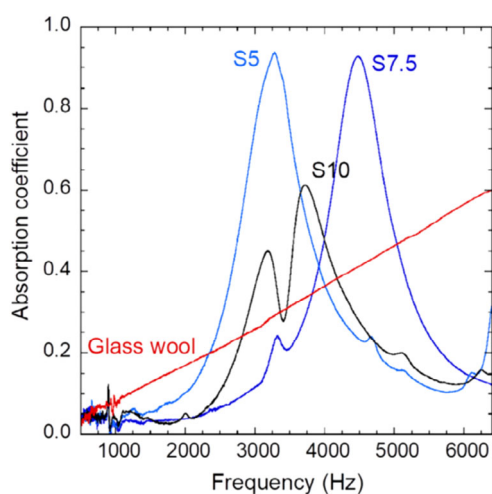


**Figure 20.** Frequency dependence of the normal-incidence sound absorption coefficient of chitosan aerogels and glass wool.<sup>[110]</sup> (Reprinted from.<sup>[110]</sup> Copyright 2019, with permission from Elsevier).

The authors suggest that a porous material with thick fibers of diameter larger than 3  $\mu\text{m}$ , which is the case of glass fibers, show

typical sound absorption profile, while the material with thinner fibers (case of aerogel) show absorption peaks due to sample vibration. The latter becomes the dominant absorption mode, resulting in the peak-shaped profiles. The position of the peak should, theoretically, depend on the density, provided the material is homogeneous which seems not to be the case for S10 (see Figure 20). Static air flow resistivity of samples S5, S7.5, and S10 was  $8.1 \times 10^{10}$ ,  $1.5 \times 10^{11}$ , and  $3.6 \times 10^{11} \text{ N s m}^{-4}$  for, respectively, for glass wool the values are much lower,  $5 \times 10^4 \text{ N s m}^{-4}$ . The high values obtained on chitosan aerogels were attributed to their mesoporous structure.

Cellulose in different forms was used to make various porous materials. For example, cellulose and lignin were dissolved in ionic liquid 1-butyl-3-methylimidazolium chloride (BmimCl) and freeze-dried from tert-butanol.<sup>[111]</sup> Upon the increase of lignin fraction, density strongly increased (from 0.024 to  $0.423 \text{ g cm}^{-3}$ ) and specific surface area decreased (from 269 to  $5 \text{ m}^2 \text{ g}^{-1}$ ). Most probably, this is because lignin is not making a self-standing network. Sound absorption was measured with a JIZB standing wave tube absorption coefficient test system (Figure 21a). Another example of sound absorption property (obtained with SW477 impedance tube) of a porous cellulose-based material prepared via cellulose dissolution and freeze-

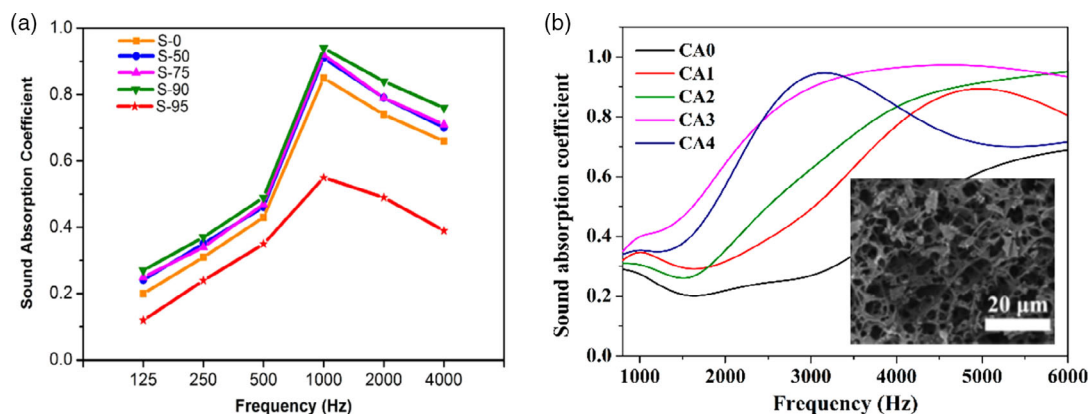


**Figure 21.** Frequency dependence of the sound absorption coefficient of porous materials obtained from dissolved cellulose: a) cellulose-lignin aerogel-like material (S-0 to S-95 correspond to samples with zero lignin to increasing lignin concentration, respectively)<sup>[111]</sup> and b) cellulose-aluminum hydroxide nanoparticles with example of morphology of CA3 sample.<sup>[112]</sup> (Reprinted with permission.<sup>[112]</sup> Copyright 2018 American Chemical Society).

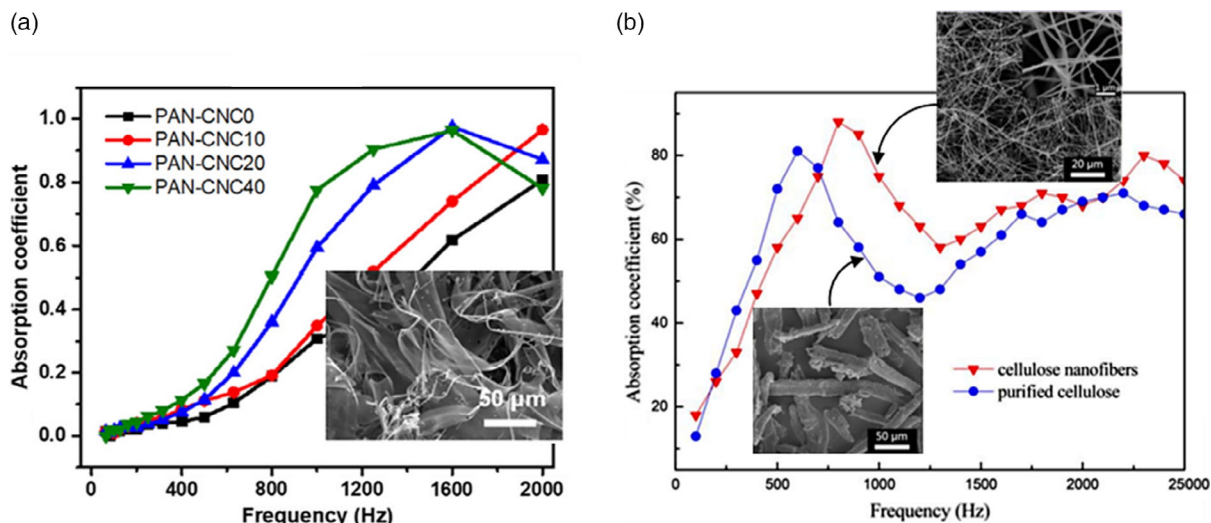


**Figure 22.** Sound absorption coefficient of a) PAN-CNC (SEM image corresponds to PAN-CNC40)<sup>[113]</sup> (Adapted from.<sup>[113]</sup> Copyright 2021, with permission from Elsevier) and b) cellulose fibers from bamboo leaves (“purified cellulose”) and the corresponding nanofibrillated cellulose<sup>[114]</sup> (Adapted from.<sup>[114]</sup> Copyright 2018, with permission from Wiley).

drying is shown in Figure 21b.<sup>[112]</sup> Cellulose was dissolved in NaOH–urea–water solvent, and aluminum hydroxide nanoparticles were formed inside cellulose network. Density increased with the increase of aluminum hydroxide from  $0.18 \text{ g cm}^{-3}$  for the neat cellulose (sample CA0 in Figure 21b) to  $0.45 \text{ g cm}^{-3}$  for cellulose filled with nanoparticles (sample CA4 in Figure 21b). Specific surface area was not reported, thus making it difficult to draw conclusions of the impact of the morphology on sound absorption properties.

Finally, few authors have reported sound absorption of nanocellulose-based porous materials. Unfortunately, none of them report specific surface area. Figure 22a shows sound absorption of freeze-dried polyacrylonitrile (PAN)-cellulose nanocrystal (CNC) material of various CNC concentrations<sup>[113]</sup> and Figure 22b of silanized nanofibrillated cellulose freeze-dried from tert-butanol.<sup>[114]</sup> “Purified cellulose” in Figure 22b corresponds to the initial fibers from bamboo leaves from which nanofibrillated cellulose was obtained, higher the CNC concentration, higher the absorption coefficient (compare PAN-CNC0 with PAN-CNC40, Figure 22a). As for the “purified cellulose” and the corresponding nanofibrillated cellulose, the absorption peaks were obtained at rather low frequency. This result is similar to the acoustic properties of cellulose-lignin porous materials (Figure 22a).

In the view of very small amount of publications reporting the acoustic properties of bio-aerogels and, except chitosan aerogels, their poor characterization, no trend can be deduced. This area, which is extremely interesting both from the fundamental and practical points of view, remains unexplored.

## 7. Discussion

In the field of noise control, there is a need for durable, safe, light weight, and also thin insulators with sound absorption (or sound insulating) capacity competing with or even exceeding the current commercial sound absorbing materials, such as rock,

mineral, and glass wools. In this review, we described how aerogels, having the inherent characteristics encompassing very low density and very high specific surface area thus maximizing the ability of the air molecules to interact with the solid frame, can provide solutions for future acoustic insulation materials. Table 3 summarizes the main types and characteristics of various aerogels together with their sound insulation properties, advantages, potential drawbacks, and open questions.

Silica aerogels are the most extensively studied among the inorganic aerogels from all perspectives: thermal, mechanical, and also for their acoustic properties. The classical silica aerogels, which are more brittle, have shown to perform as excellent acoustic insulation solutions as beads or granules and in the form of glazing systems for building insulation. For applications that require better vibrational properties, such as aircraft and automotive applications, flexible silica aerogel sheets, or blankets perform similar or better as compared to the state-of-the-art sound insulation materials, especially in the low-frequency region. Optimization techniques to tailor the synthesis and, subsequently, the structural properties of silica aerogels to target acoustic insulation requirements are missing. However, since the acoustic properties, like their thermal and mechanical properties, scale with the density of the aerogels, the know-how from optimization of other-than-acoustic properties could play an important role in accelerating the development of high-performance sound-insulating aerogels. This is where theoretical development in describing the acoustic properties of aerogels are urgently needed to accelerate the reverse engineering of the materials development process. Moreover, scalability of silica aerogels is now well established (for example, Spaceloft or Cryogel from Aspen).

Polymer aerogels have reached a certain maturity level to be produced via a cost-efficient manufacturing process (e.g., polymer aerogel continuous manufacturing) and may have potential for commercial acoustic insulation applications provided that supercritical drying is avoided. Polymer aerogels are structurally

**Table 3.** A brief summary of the acoustic properties, open questions, and needs related to different types of aerogels.

Aerogel class	Main characteristics	What is known about acoustic properties?	Disadvantages	Open questions/needs to advance
Inorganic (silica based) and their composites	Most well-studied aerogels that are extremely light-weight, manufacturable as monoliths, beads (granules), and sheets, can be transparent or translucent, can be brittle or flexible, reinforced using hybrid (crosslinking), or composite (with fibers, blankets) approaches. Drying in supercritical conditions can be avoided	There is a certain set of experimental data on the acoustic properties of silica aerogels. Both sound absorption and sound transmission losses have been studied for aerogel monoliths, beads, and sheets (blankets). Silica aerogels possess better acoustic insulation performance than state of the art materials, e.g., glass wool, in the low-frequency regime. Theoretical models moderately well describe the acoustic properties of silica aerogels. Potential applications were suggested for aircraft cabin insulation and in glazing systems for building insulation.	Humidity sensitivity needs chemical treatments (they can be the same as used for thermal insulation). Still expensive because of the requirements to the starting silica	Need in reverse engineering (optimization) of synthesis parameters to target for acoustic properties. Since all, acoustic, thermal, and mechanical properties scale with density, it is important to establish a trade-off between the structural parameters and target properties. Theoretical quantitative models are needed to understand and predict the acoustic properties of silica aerogels.
Synthetic polymer	Low density and rather high specific surface area. Low manufacturing cost and excellent mechanical properties such as high ductility and strength. Synthesized mainly as monoliths. Drying in supercritical conditions can be avoided but not developed on the pilot or industrial scale.	Both sound absorption and sound transmission loss have been experimentally studied for some of the common polymer aerogels	Most of aerogels are still made using drying with supercritical CO <sub>2</sub> Some synthesis routes involve environmentally unfriendly compounds. Emission of toxic gases when burning. Limited applicability at high temperatures (above 300 °C) due to polymer degradation. There are exceptions such as polyimides as high-performance polymers of which decomposition starts at 500 °C, but there is no acoustic data reported yet.	Upscaling of processing routes avoiding high-pressure drying for any type of polymeric aerogel. More experimental evidence on the acoustic properties. Developing and testing theoretical approaches. As the polymer material properties can be significantly affected by temperature, there is a need in the studies of the acoustic properties of polymer aerogels at low and high temperatures.
Bio-based	Low density and rather high surface area. No “synthesis” is required as bio-aerogels are made from natural polymers. Possibility of fabricating composite inorganic/bio-based aerogels. Easy to make of any shape, from monoliths to microparticles. Good mechanical properties (no breakage under compression). The majority of bio-aerogels are biodegradable	No established knowledge covering the acoustic properties of bio-aerogels	Highly sensitive to humidity. Need in solvent exchange which is a slow (diffusion driven) process. Majority of processing routes involve drying with supercritical CO <sub>2</sub> . Low resistance to fire unless pre-treated. Very poor knowledge on the acoustic properties	Experimental basis and theoretical approaches need to be developed.

durable and theoretically can serve as an ultralight alternative to the state-of-the-art acoustic impellers with superior sound transmission loss capabilities. The superiority of polymer aerogels over silica aerogels is in their acoustic impedance characteristics. Unlike silica aerogels with extremely small pore sizes, polymer aerogels allow a better energy transfer between the air molecules and the aerogel structure making them a better acoustic absorber compared to silica aerogels. Acoustic damper is another prospective application of polymer aerogels in a composite form that can potentially be constructed in conjunction with an acoustic absorber (e.g., melamine, gypsum, etc.). In this way, the absorber captures the air molecule energy and transfer it to the aerogel solid structure for acoustic damping.

Bio-aerogels are “young” materials that started to be developed at the beginning of the 21st century. Till now, the majority is based on polysaccharides, the “synthesis” of which is controlled by Nature. A huge number of parameters related to polysaccharides themselves and to numerous different processing conditions result in a rather poor understanding of bio-aerogels’ polymer–structure–properties relationships. Bio-aerogels are very attractive materials as they are based on renewable feedstock with no toxic compound used; however, till now, the acoustic properties of bio-aerogels are unexplored.

In order to advance the theoretical interpretation of the acoustic properties of aerogels, the following aspects should be considered. 1) theoretical interpretation using the Biot’s dynamic theory of poroelasticity has shown some success in the prediction of the polyurea aerogel sound transmission loss behavior; however, there is still a need to establish a direct microstructure–property relationship through a micromechanical model for the interpretation of sound wave interactions with aerogels of different hierarchical micro/nanostructures. 2) based on the JCA model, an inverse characterization method was applied to determine characteristic material parameters of silica aerogel granules complying with the JCA model and with values listed in literature. A specific combination of physically realistic parameters led to an optimal fit between theoretical and experimental sound absorption curves. This opens up the potential of further extending/modifying either the theoretical implications or the theory itself to describe the acoustic properties other (nonsilica) aerogels. Generalizing micromechanical models for aerogels can be very challenging, as the morphological features of diverse aerogels are different, e.g., fibrillar, particle-aggregated, hierarchical. However, tuning or extending the JCA model, which is semi-empirical, can certainly pave a way for developing a generalized model for describing the sound absorption properties in aerogels.

## 8. Conclusions

The overview of the acoustic properties of aerogels shows their great potential in sound insulation. To date, the characterization and understanding of the acoustic behavior are limited mainly to inorganic (silica-based) aerogels and their composites rather than to polymer aerogels, synthetic or bio-based. Silica-based aerogels have demonstrated excellent sound absorption over a wide range of frequencies. Typically, conventional porous materials do not show exceptional insulation characteristics in the low-frequency

range, below 200 Hz, where silica and some synthetic polymer aerogels have outperformed any state-of-the-art insulation material. Moreover, for the frequency range up to 5 kHz, aerogels show significantly higher sound transmission loss properties (e.g., 40 dB cm<sup>-1</sup> for monolithic polyurea aerogels at 0.45 g cm<sup>-3</sup> bulk density) compared to traditional state-of-the-art acoustics materials, such as polyurethane foam at similar density, which can only reach up to 5 dB. This is another breakthrough for aerogels that makes them different from other porous materials. However, silica aerogels possess some drawbacks (e.g., the price) that hinder, for the time being, their commercialization. Bio-based polymer aerogels are awaiting to be explored for their acoustic properties.

The interpretation of the experimental results requires the development of new and/or adjusted theoretical approaches. Well-established models such as the Johnson–Champoux–Allard model have shown potential in correlating physical properties of silica aerogels to their sound absorption characteristics, thus opening a door for the understanding and predicting the acoustic properties of polymer-based aerogels.

Overall, the field of aerogels for acoustic applications is open for developments in all its sectors and from different starting materials, organic or inorganic, and/or their composites. Since early-stage material development often proceeds with quite small samples, unifying measurement standards for small batches of new materials between different laboratories would definitely benefit the field as a whole. In addition, the detailed characterization of aerogel parameters, including porosity, pore size distribution, and specific surface area, is necessary to have enough data for establishing structure–function relationships, especially in the young and emerging fields, such as bio-aerogels. To summarize, an in-depth systematic experimental and theoretical investigations of a broad range of aerogels are needed to advance the development of high-performance materials for acoustic insulation.

## Acknowledgements

This work was supported and carried out in the framework of COST Action CA18125 “Advanced Engineering and Research of aeroGels for Environment and Life Sciences” (AERoGELS, <https://www.cost.eu/actions/CA18125>), funded by the European Commission. The authors thank Noora Jääntti (Aalto University) for technical help. H.L. acknowledges the support of the U.S. Department of Energy’s National Nuclear Security Administration under contracts DE-NA-0003525 and DE-NA0003962 and the Louis A. Beecherl Jr. Endowed Chair. S.M. would like to thank the United States National Aeronautics and Space Administration (NASA) Postdoctoral Program at the NASA Glenn Research Center, administered by Oak Ridge Associated Universities under contract with NASA. A.R. and B.M. acknowledge the support of the Program Directorate Aeronautics of the German Aerospace Center (Project: Innovative Digital Cabin Design – InDiCaD). J.V. acknowledges funding from Academy of Finland’s Flagship Program under Project Nos. 318890 and 318891 (Competence Center for Materials Bioeconomy and FinnCERES). S.V. acknowledges the support of the NASA Space Technology Mission Directorate (STMD).

## Conflict of Interest

The authors declare no conflict of interest.



## Keywords

silica aerogels, acoustic properties, bio-aerogels, composite aerogels, polymer aerogels

Received: August 5, 2022  
Revised: October 18, 2022  
Published online:

- [1] F. Schwertfeger, D. Frank, M. Schmidt, *J. Non-Cryst. Solids* **1998**, 225, 24.
- [2] X. Tang, X. Yan, *Composites, Part A* **2017**, 101, 360.
- [3] C. M. Wu, M. H. Chou, *Eur. Polym. J.* **2016**, 82, 35.
- [4] C. Lang, J. Fang, H. Shao, X. Ding, T. Lin, *Nat. Commun.* **2016**, 7, 11108.
- [5] R. Liu, L. Hou, G. Yue, H. Li, J. Zhang, J. Liu, B. Miao, N. Wang, J. Bai, Z. Cui, T. Liu, Y. Zhao, *Adv. Fiber Mater.* **2022**, 4, 604.
- [6] X. Li, Y. Peng, Y. He, C. Zhang, D. Zhang, Y. Liu, J. Lee, M.-Y. Li, X. Li, Y. Peng, Y. He, C. Zhang, D. Zhang, Y. Liu, *Nanomaterials* **2022**, 12, 1123.
- [7] C. Lang, J. Fang, H. Shao, X. Ding, T. Lin, *Mater. Today: Proc.* **2017**, 4, 5306.
- [8] M. A. Kuczmarski, J. C. Johnston, *Acoustic Absorption in Porous Materials*, NASA, Glenn Research Center, Cleveland, OH **2011**.
- [9] F. Bechwati, M. R. Avis, D. J. Bull, T. J. Cox, J. A. Hargreaves, D. Moser, D. K. Ross, O. Umnova, R. Venegas, *J. Acoust. Soc. Am.* **2012**, 132, 239.
- [10] U. Berardi, G. Iannace, *Build. Environ.* **2015**, 94, 840.
- [11] Markets and Markets, *Acoustic Insulation Market Global Forecast to 2026*, Markets and Markets, IL **2021**.
- [12] F. Zangeneh-Nejad, R. Fleury, *Rev. Phys.* **2019**, 4, 100031.
- [13] F. Fahy, *Foundations of Engineering Acoustics*, Academic Press, London, UK **2000**.
- [14] M. A. Aegerter, N. Leventis, M. Koebel, S. A. Steiner III, *Handbook of Aerogels*, In Series Springer Handbooks, Springer Nature Switzerland AG **2023**, ISSN 2522–8692.
- [15] S. S. Kistler, *Nature* **1931**, 127, 741.
- [16] S. S. Kistler, *J. Phys. Chem.* **1932**, 36, 52.
- [17] S. J. Teichner, G. A. Nicolaon, US3672833A, **1972**.
- [18] R. J. Ayen, P. A. Iacobucci, *Rev. Chem. Eng.* **1988**, 5, 157.
- [19] R. W. Pekala, *J. Mater. Sci.* **1989**, 24, 3221.
- [20] J. C. Williams, M. A. B. Meador, L. McCorkle, C. Mueller, N. Wilmoth, *Chem. Mater.* **2014**, 26, 4163.
- [21] H. Guo, M. A. B. Meador, L. McCorkle, D. J. Quade, J. Guo, B. Hamilton, M. Cakmak, G. Sprowl, *ACS Appl. Mater. Interfaces* **2011**, 3, 546.
- [22] A. Rigacci, J. C. Marechal, M. Repoux, M. Moreno, P. Achard, *J. Non-Cryst. Solids* **2004**, 350, 372.
- [23] T. Budtova, D. A. Aguilera, S. Beluns, L. Berglund, C. Chartier, E. Espinosa, S. Gaidukovs, A. Klimek-Kopyra, A. Kmita, D. Lachowicz, F. Liebner, O. Platnieks, A. Rodríguez, L. K. T. Navarro, F. Zou, S. J. Buwalda, *Polymers* **2020**, 12, 2779.
- [24] S. Zhao, W. J. Malfait, N. Guerrero-Alburquerque, M. M. Koebel, G. Nyström, *Angew. Chem., Int. Ed.* **2018**, 57, 7580.
- [25] S. Malakooti, H. G. Churu, A. Lee, T. Xu, H. Luo, N. Xiang, C. Sotiriou-Leventis, N. Leventis, H. Lu, *J. Non-Cryst. Solids* **2017**, 476, 36.
- [26] S. Malakooti, G. Qin, C. Mandal, R. Soni, T. Taghvaei, Y. Ren, H. Chen, N. Tsao, J. Shiao, S. S. Kulkarni, C. Sotiriou-Leventis, N. Leventis, H. Lu, *ACS Appl. Polym. Mater.* **2019**, 1, 2322.
- [27] L. Druel, T. Budtova, FR3094009A1, **2019**.
- [28] M. Perrut, E. Francais, US5962539A, **1999**.
- [29] N. Hüsing, U. Schubert, R. Mezei, P. Fratzl, B. Riegel, W. Kiefer, D. Kohler, W. Mader, *Chem. Mater.* **1999**, 11, 451.
- [30] S. Groult, T. Budtova, *Eur. Polym. J.* **2018**, 108, 250.
- [31] C. Tan, B. M. Fung, J. K. Newman, C. Vu, *Adv. Mater.* **2001**, 13, 644.
- [32] S. Malakooti, M. I. Hatamleh, R. Zhang, T. Taghvaei, M. Miller, Y. Ren, N. Xiang, D. Qian, C. Sotiriou-Leventis, N. Leventis, H. Lu, *Soft Matter* **2021**, 17, 4496.
- [33] M. A. B. Meador, C. R. Alemán, K. Hanson, N. Ramirez, S. L. Vivod, N. Wilmoth, L. McCorkle, *ACS Appl. Mater. Interfaces* **2015**, 7, 1240.
- [34] N. Leventis, C. Sotiriou-Leventis, G. Zhang, A.-M. M. Rawashdeh, *Nano Lett.* **2002**, 1, 957.
- [35] M. A. B. Meador, E. F. Fabrizio, F. Ilhan, A. Dass, G. Zhang, P. Vassilaras, J. C. Johnston, N. Leventis, *Chem. Mater.* **2005**, 17, 1085.
- [36] A. Katti, N. Shimpi, S. Roy, H. Lu, E. F. Fabrizio, A. Dass, L. A. Capadona, N. Leventis, *Chem. Mater.* **2006**, 18, 285.
- [37] S. Aney, J. Schettler, M. Schwan, B. Milow, A. Rege, *Adv. Eng. Mater.* **2022**, 24, 2100095.
- [38] S. Malakooti, S. Rostami, H. G. Churu, H. Luo, J. Clark, F. Casarez, O. Rettenmaier, S. Daryadel, M. Minary-Jolandan, C. Sotiriou-Leventis, N. Leventis, H. Lu, *RSC Adv.* **2018**, 8, 21214.
- [39] S. Malakooti, S. L. Vivod, M. Pereira, C. R. Ruggeri, D. M. Revilock, R. Zhang, H. Guo, D. A. Scheiman, L. S. McCorkle, H. Lu, *Sci. Rep.* **2022**, 12, 13933.
- [40] L. J. Gibson, M. F. Ashby, *Cellular Solids: Structure and Properties* (2nd ed., Cambridge Solid State Science Series), Cambridge University Press, Cambridge **1999**.
- [41] J. Gross, J. Fricke, *NanoStruct. Mater.* **1995**, 6, 905.
- [42] R. Abdusalamov, C. Scherdel, M. Itskov, B. Milow, G. Reichenauer, A. Rege, *J. Phys. Chem. B* **2021**, 125, 1944.
- [43] R. W. Pekala, C. T. Alviso, J. D. LeMay, *J. Non-Cryst. Solids* **1990**, 125, 67.
- [44] T. Budtova, *Cellulose* **2019**, 26, 81.
- [45] N. Buchtová, C. Pradille, J.-L. Bouvard, T. Budtova, *Soft Matter* **2019**, 15, 7901.
- [46] R. Chandrasekaran, M. Hillgärtner, K. Ganesan, B. Milow, M. Itskov, A. Rege, *Sci. Rep.* **2021**, 11, 10198.
- [47] S. Aney, A. Rege, *Math. Mech. Solids* **2022**, 108128652211241, <https://doi.org/10.1177/10812865221124142>.
- [48] R. Baetens, B. P. Jelle, A. Gustavsen, *Energy Build* **2011**, 43, 761.
- [49] D. M. Smith, A. Maskara, U. Boes, *J. Non-Cryst. Solids* **1998**, 225, 254.
- [50] G. Markevicius, R. Ladj, P. Niemeyer, T. Budtova, A. Rigacci, *J. Mater. Sci.* **2017**, 52, 2210.
- [51] X. Lu, M. C. Arduini-Schuster, J. Kuhn, O. Nilsson, J. Fricke, R. W. Pekala, *Science* **1992**, 255, 971.
- [52] S. Groult, T. Budtova, *Carbohydr. Polym.* **2018**, 196, 73.
- [53] F. Zou, T. Budtova, *Carbohydr. Polym.* **2021**, 266, 118130.
- [54] Y. Kobayashi, T. Saito, A. Isogai, Y. Kobayashi, A. T. Saito, A. Isogai, *Angew. Chem., Int. Ed.* **2014**, 53, 10394.
- [55] Z. Mazrouei-Sebdani, H. Begum, S. Schoenwald, K. V. Horoshenkov, W. J. Malfait, *J. Non-Cryst. Solids* **2021**, 562, 120770.
- [56] M. Gronauer, A. Kadur, J. Fricke, in *Aerogels. Springer Proceedings in Physics*, Vol. 6 (Ed: J. Fricke), Springer, Berlin, Heidelberg **1986**, p. 167.
- [57] J. Gross, R. Goswin, R. Gerlach, J. Fricke, *J. Phys. D: Appl. Phys.* **1988**, 21, 1447.
- [58] J. Gross, J. Fricke, *J. Acoust. Soc. Am.* **1992**, 91, 2004.
- [59] J. Fricke, X. Lu, P. Wang, D. Büttner, U. Heinemann, *Int. J. Heat Mass Transfer* **1992**, 35, 2305.
- [60] L. Weigold, G. Reichenauer, *J. Non-Cryst. Solids* **2014**, 406, 73.
- [61] J. Gross, J. Fricke, L. W. Hrubesh, *J. Acoust. Soc. Am.* **1992**, 91, 2004.

- [62] V. Gibiat, O. Lefeuvre, T. Woignier, J. Pelous, J. Phalippou, *J. Non-Cryst. Solids* **1995**, 186, 244.
- [63] J. F. T. Conroy, B. Hosticka, S. C. Davis, A. N. Smith, P. M. Norris, *Microscale Thermophys. Eng.* **1999**, 3, 199.
- [64] L. Forest, V. Gibiat, A. Hooley, *J. Non-Cryst. Solids* **2001**, 285, 230.
- [65] C. D. Smith, T. L. Parrott, *J. Acoust. Soc. Am.* **1983**, 74, 1577.
- [66] P. Ricciardi, V. Gibiat, A. Hooley, *Forum Acusticum*, EAA, Spain **2002**.
- [67] C. Buratti, F. Merli, E. Moretti, *Energy Build.* **2017**, 152, 472.
- [68] H. Begum, K. V. Horoshenkov, M. Conte, W. J. Malfait, S. Zhao, M. M. Koebel, P. Bonfiglio, R. Venegas, *J. Acoust. Soc. Am.* **2021**, 149, 4149.
- [69] R. Venegas, C. Boutin, O. Umnova, *Phys. Fluids* **2017**, 29, 082006.
- [70] Y. Abawi, F. Langfeldt, W. Gleine, B. Milow, in *DAGA 2020*, **2020**.
- [71] F. Merli, A. M. Anderson, M. K. Carroll, C. Buratti, *Appl. Acoust.* **2018**, 142, 123.
- [72] W. Jichao, S. Jun, X. Y. Ni, B. Wang, X. Wang, J. Li, *Rare Met. Mater. Eng.* **2010**, 39, 14.
- [73] Y. Xie, J. Beamish, *Phys. Rev. B* **1998**, 57, 3406.
- [74] D. R. Daughton, J. MacDonald, N. Mulders, *J. Non-Cryst. Solids* **2003**, 319, 297.
- [75] J. Lin, G. Li, W. Liu, R. Qiu, H. Wei, K. Zong, X. Cai, *J. Mater. Sci.* **2021**, 56, 10812.
- [76] Z. Talebi, P. Soltani, N. Habibi, F. Latifi, *Constr. Build. Mater.* **2019**, 220, 76.
- [77] K. W. Oh, D. K. Kim, S. H. Kim, *Fibers and Polym.* **2009**, 10, 731.
- [78] M. Ramamoorthy, A. A. Pisal, R. S. Rengasamy, A. V. Rao, *J. Porous Mater.* **2018**, 25, 179.
- [79] H. Begum, K. V. Horoshenkov, *Appl. Sci.* **2021**, 11, 4593.
- [80] K. V. Horoshenkov, A. Hurrell, J.-P. Groby, *J. Acoust. Soc. Am.* **2019**, 145, 2512.
- [81] N. Eskandari, S. Motahari, Z. Atoufi, G. Hashemi Motlagh, M. Najafi, *J. Appl. Polym. Sci.* **2017**, 134, 44685.
- [82] S. B. Riffat, G. Qiu, *Int. J. Low-Carbon Technol.* **2013**, 8, 1.
- [83] F. Cotana, A. L. Pisello, E. Moretti, C. Buratti, *Build. Environ.* **2014**, 81, 92.
- [84] A. Wood, *A Textbook of Sound : Being An Account of the Physics of Vibrations with Special Reference to Recent Theoretical and Technical Developments*, Bell, London **1941**.
- [85] M. A. Biot, *J. Acoust. Soc. Am.* **1956**, 28, 168.
- [86] M. A. Biot, *J. Acoust. Soc. Am.* **1956**, 28, 179.
- [87] D. L. Johnson, J. Koplik, R. Dashen, D. L. Johnson, J. Koplik, R. Dashen, *J. Fluid Mech.* **1987**, 176, 379.
- [88] Y. Champoux, J. F. Allard, *J. Appl. Phys.* **1991**, 70, 1975.
- [89] J. F. Allard, *J. Acoust. Soc. Am.* **1992**, 91, 3346.
- [90] E. P. Barrett, L. G. Joyner, P. P. Halenda, *J. Am. Chem. Soc.* **1951**, 73, 373.
- [91] C. Hesse, P. Allebrodt, A. Rege, *Deutsche Gesellschaft Für Luft- Und Raumfahrt - Lilienthal-Oberth E.V.*, Bonn **2020**.
- [92] D. Lafarge, P. Lemarinier, J. F. Allard, V. Tarnow, *J. Acoust. Soc. Am.* **1997**, 102, 1995.
- [93] S. R. Pride, F. D. Morgan, A. F. Gangi, *Phys. Rev. B: Condens. Matter* **1993**, 47, 4964.
- [94] T. Taghvaei, S. Donthula, P. M. Rewatkar, H. Majedi Far, C. Sotiriou-Leventis, N. Leventis, *ACS Nano* **2019**, 13, 3677.
- [95] S. Donthula, C. Mandal, J. Schisler, T. Leventis, M. A. B. Meador, C. Sotiriou-Leventis, N. Leventis, *ACS Appl. Mater. Interfaces* **2018**, 10, 23321.
- [96] M. Papastergiou, A. Kanellou, D. Chriti, G. Raptopoulos, P. Paraskevopoulou, *Materials* **2018**, 11, 2249.
- [97] M. A. B. Meador, E. J. Malow, R. Silva, S. Wright, D. Quade, S. L. Vivod, H. Guo, J. Guo, M. Cakmak, *ACS Appl. Mater. Interfaces* **2012**, 4, 536.
- [98] B. N. Nguyen, M. A. B. Meador, D. Scheiman, L. McCorkle, *ACS Appl. Mater. Interfaces* **2017**, 9, 27313.
- [99] C. Chidambareswarapattar, L. Xu, C. Sotiriou-Leventis, N. Leventis, *RSC Adv.* **2013**, 3, 26459.
- [100] R. Yao, Z. Yao, J. Zhou, *Mater. Lett.* **2016**, 176, 199.
- [101] N. Leventis, C. Sotiriou-Leventis, N. Chandrasekaran, S. Mulik, Z. J. Larimore, H. Lu, G. Churu, J. T. Mang, *Chem. Mater.* **2010**, 22, 6692.
- [102] N. Leventis, C. Sotiriou-Leventis, S. Mulik, US10301445B2, **2011**.
- [103] M. A. Price, T. D. Aslam, J. J. Quirk, in *AIP Conf. Proc.*, American Institute of Physics Inc., Melville, NY **2018**, p. 110016.
- [104] N. Whitworth, B. Lambourn, in *AIP Conf. Proc.*, American Institute Of Physics Inc., Melville, NY **2018**, p. 030007.
- [105] S. Malakooti, H. G. Churu, A. Lee, S. Rostami, S. J. May, S. Ghidai, F. Wang, Q. Lu, H. Luo, N. Xiang, C. Sotiriou-Leventis, N. Leventis, H. Lu, *Adv. Eng. Mater.* **2018**, 20, 1700937.
- [106] ASTM E90-09, Standard Test Method for Laboratory Measurement of Airborne Sound Transmission Loss of Building Partitions and Elements **2016**.
- [107] ISO 10140-1, Acoustics - Laboratory Measurement of Sound Insulation of Building Elements **2010**.
- [108] F. Fahy, P. Gardonio, *Sound and Structural Vibration*, Academic Press, Oxford **2007**.
- [109] M. Rapisarda, G. P. Malfense Fierro, M. Meo, *Sci. Rep.* **2021**, 11, 10572.
- [110] S. Takeshita, S. Akasaka, S. Yoda, *Mater. Lett.* **2019**, 254, 258.
- [111] C. Wang, Y. Xiong, B. Fan, Q. Yao, H. Wang, C. Jin, Q. Sun, *Sci. Rep.* **2016**, 6, 32383.
- [112] C. He, J. Huang, S. Li, K. Meng, L. Zhang, Z. Chen, Y. Lai, *ACS Sustainable Chem. Eng.* **2018**, 6, 927.
- [113] L. Cao, X. Yu, X. Yin, Y. Si, J. Yu, B. Ding, *J. Colloid Interface Sci.* **2021**, 597, 21.
- [114] B. Fan, Q. Yao, C. Wang, C. Jin, H. Wang, Y. Xiong, S. Li, Q. Sun, *Polym. Compos.* **2018**, 39, 3869.
- [115] S. Mulik, C. Sotiriou-Leventis, L. N. Leventis, *Chem. Mater.* **2007**, 19, 6138.
- [116] N. Buchtová, T. Budtova, *Cellulose* **2016**, 23, 2585.
- [117] A. Demilecamps, G. Reichenauer, A. Rigacci, T. Budtova, *Cellulose* **2014**, 21, 2625.
- [118] H. Guo, M. Ann, B. Meador, L. S. Mccorkle, D. A. Scheiman, J. D. Mccrone, B. Wilkewitz, *RSC Adv.* **2016**, 6, 26055.
- [119] S. Caponi, A. Fontana, M. Montagna, O. Pilla, F. Rossi, F. Terki, T. Woignier, *J. Non-Cryst. Solids* **2003**, 322, 29.
- [120] X. Li, Z. Yang, K. Li, S. Zhao, Z. Fei, Z. Zhang, *J. Sol-Gel Sci. Technol.* **2019**, 92, 652.
- [121] E. Moretti, F. Merli, E. Cuce, C. Buratti, *Energy Procedia* **2017**, 111, 472.
- [122] M. Venkataraman, R. Mishra, V. Arumugam, H. Jamshaid, J. Militky, in *Proc. Nanocon 2014*, Brno, Czech Republic **2014**, p. 124.
- [123] T. Yang, X. Xiong, M. Venkataraman, R. Mishra, J. Novák, J. Militky, *J. Text. Inst.* **2018**, 110, 196.
- [124] P. Yan, B. Zhou, A. Du, *RSC Adv.* **2014**, 4, 58252.
- [125] M. Hamidi, P. Nassiri, H. A. Panahi, L. Taghavi, S. Bazgir, *Polym. Polym. Compos.* **2021**, 29, 57.
- [126] Y. Salissou, R. Panneton, O. Doutres, *J. Acoust. Soc. Am.* **2012**, 131, EL216.
- [127] ASTM E1050-12, Standard Test Method for Impedance and Absorption of Acoustical Materials Using a Tube Two Microphones and a Digital Frequency Analysis System **2012**.
- [128] ASTM E2611-19, Standard Test Method for Normal Incidence Determination of Porous Material Acoustical Properties Based on the Transfer Matrix Method **2019**.



**Tatiana Budtova** is an expert in polymer chemical physics, in particular, in polymer solutions, gels, and aerogels with the focus on biomass-based polymers and also in polymer composites with natural fibers. She defended her Ph.D. in the Institute of Macromolecular Compounds of Russian Academy of Sciences and got Habilitation in France. She holds “research director” position in the Center for Materials Forming of Mines Paris, France, and she is the leader of “Biobased Polymers and Composites” group. She is editor-in-chief of *Carbohydrate Polymers* journal, and in 2020, she was awarded a “silver medal” by CNRS for the outstanding research on bioaerogels.



**Tapio Lokki** has studied acoustics, audio signal processing, and computer science at the Helsinki University of Technology (TKK) and received a M.Sc. degree in 1997 and a D.Sc. (Tech.) degree in 2002. Prof. Lokki leads his virtual acoustics team to create novel objective and subjective ways to evaluate room acoustics, especially concert halls. In addition, the team currently contributes to sound rendering algorithms for virtual reality applications and novel wood fibre-based absorption materials. Prof. Lokki is a fellow of the AES and an honorary member of the Acoustical Society of Finland.



**Sadeq Malakooti** is a NASA research fellow in the Materials and Structures Division at the NASA Glenn Research Center in Cleveland, Ohio. Sadeq received his Ph.D. in Mechanical Engineering from The University of Texas at Dallas in 2020. He is a subject matter expert in the dynamic properties of polymer aerogels and composites under extreme conditions. Dr. Malakooti is an active member of the Society for Experimental Mechanics.



**Ameya Rege** is a group leader for Atomistic and Microstructure Simulations at the Department of Aerogels and Aerogel Composites of the Institute of Materials Research at the German Aerospace Center (DLR). He is also a visiting senior lecturer (associate professor) at the School of Computer Science and Mathematics of the Keele University, UK He completed his Ph.D. at the RWTH Aachen University in 2018. He pursues research in multiscale materials modeling of soft materials and high-performance materials simulations.



**Hongbing Lu** is a professor and Louis A. Beecherl Jr. chair of Mechanical Engineering at University of Texas at Dallas. He received his Ph.D. in Aeronautics from Caltech, M.S. in Engineering Mechanics at Tsinghua University, and B.S. in Solid Mechanics at Huazhong University of Science and Technology. He specializes in experimental mechanics of time-dependent materials, including aerogels, polymers, and composites. He is a fellow of ASME (American Society of Mechanical Engineers) and SEM (Society for Experimental Mechanics). He is the editor-in-chief for *Mechanics of Time-Dependent Materials* and an associate technical editor for *Experimental Mechanics*.



**Barbara Milow** is the leader of the Department of Aerogels and Aerogel Composites of the Institute of Materials Research at the German Aerospace Center (DLR). Here, Prof. Dr. Milow follows the research and development of aerogel materials from laboratory to technical scale for lightweight construction, thermal and acoustic insulation, and energy storage applications. Since 2018, she is a full professor at the University of Cologne, Germany. In 2020, she also became an Honorary Affiliate Member of the University of British Columbia, Canada.



**Jaana Vapaavuori** (Department of Chemistry and Materials Science, Aalto University) received her Ph.D. in Applied Physics in 2013. She leads Multifunctional Materials Design Group, established in 2019. She has received multiple recognitions, such as Banting Postdoctoral Fellowship (Canada), the Young Researcher of the Year 2020 award of Finnish Foundation of Technology Promotion, ERC Starting grant of European Research Council, and she is also leader of a Nordic Network beyond e-Textiles.



**Stephanie L. Vivod** is the technical lead for polymer aerogel group in the Materials and Structures Division at the NASA Glenn Research Center in Cleveland, Ohio. She is a subject matter expert in the synthesis and characterization of high-temperature polymers, flexible elastomeric polymer substrates, and organic, inorganic, and hybrid aerogels. Stephanie received her B.S. in Chemistry from Cleveland State University and her Ph.D. in Polymer Science from The University of Akron. Dr. Vivod is an active member of the American Chemical Society and the Materials Research Society.